Maternal nitric oxide homeostasis impacts female gametophyte development under optimal and stress conditions

Junzhe Wang , ^{1,2,†} Xiaolong Guo , ^{1,†} Yijin Chen , ¹ Tianxiang Liu , ¹ Jianchu Zhu , ¹ Shengbao Xu , ^{1,*} and Elizabeth Vierling , ^{3,*}

- 1 State Key Laboratory for Crop Stress Resistance and High-Efficiency Production, College of Agronomy, Northwest A&F University, Yangling, Shaanxi 712100, China
- 2 Hainan Yazhou Bay Seed Laboratory, Yazhou, Sanya 572025, China
- 3 Department of Biochemistry & Molecular Biology, University of Massachusetts, Amherst, MA 01003, USA

The authors responsible for distribution of materials integral to the findings presented in this article in accordance with the policy described in the Instructions for Authors (https://academic.oup.com/plcell/pages/General-Instructions) are: Shengbao Xu (xushb@nwsuaf.edu.cn) and Elizabeth Vierling (vierling@biochem.umass.edu).

Abstract

Research Article

In adverse environments, the number of fertilizable female gametophytes (FGs) in plants is reduced, leading to increased survival of the remaining offspring. How the maternal plant perceives internal growth cues and external stress conditions to alter FG development remains largely unknown. We report that homeostasis of the stress signaling molecule nitric oxide (NO) plays a key role in controlling FG development under both optimal and stress conditions. NO homeostasis is precisely regulated by S-nitrosoglutathione reductase (GSNOR). Prior to fertilization, GSNOR protein is exclusively accumulated in sporophytic tissues and indirectly controls FG development in Arabidopsis (*Arabidopsis thaliana*). In GSNOR null mutants, NO species accumulated in the degenerating sporophytic nucellus, and auxin efflux into the developing FG was restricted, which inhibited FG development, resulting in reduced fertility. Importantly, restoring *GSNOR* expression in maternal, but not gametophytic tissues, or increasing auxin efflux substrate significantly increased the proportion of normal FGs and fertility. Furthermore, *GSNOR* overexpression or added auxin efflux substrate increased fertility under drought and salt stress. These data indicate that NO homeostasis is critical to normal auxin transport and maternal control of FG development, which in turn determine seed yield. Understanding this aspect of fertility control could contribute to mediating yield loss under adverse conditions.

Introduction

Plants reduce their number of offspring in unfavorable environments, which is regarded as an evolutionary adaptive mechanism for enhancing offspring survival under adverse conditions (Melser and Klinkhamer 2001; Meyer et al. 2014). It remains unknown how the maternal plant monitors internal growth cues and external stress conditions in order to optimize the number of offspring produced (Severino 2021). Maternal control of fertility is not only critical to

species survival but is also highly relevant to agricultural production, as severe yield losses can occur when crops experience environmental stress around flowering time (Lohani et al. 2020). Thus, determining the underlying mechanisms is important for designing strategies to maximize agricultural output under environmental stress.

Female gametophyte (FG) development is a key stage at which the maternal plant can exert control of seed number and quality (Sun et al. 2004). The FG originates from a

^{*}Author for correspondence: xushb@nwsuaf.edu.cn (S.X.), vierling@biochem.umass.edu (E.V.)

[†]These authors contributed equally.

IN A NUTSHELL

Background: In adverse environments, plants often produce more nitric oxide (NO), which plays a pivotal role in modulating plant growth and development. Additionally, under stress, the number of fertilizable female gametophytes (FGs) in plants is reduced, leading to enhanced survival of the remaining offspring. The mechanisms by which the maternal plant perceives internal growth signals and external stress factors to modify FG development are still largely unknown.

Question: How does the maternal plant perceive internal growth cues and external stress conditions to regulate FG development? What are the mechanisms by which NO controls FG development?

Findings: NO homeostasis is critical for regulating FG development in Arabidopsis. NO homeostasis is precisely maintained by S-nitrosoglutathione reductase (GSNOR), an enzyme that accumulates exclusively in sporophytic tissues and indirectly governs the development of FGs prior to fertilization. Disrupted maternal NO homeostasis in *hot5* mutants or the addition of exogenous NO inhibits the delivery of maternal auxin to the FG, thereby affecting FG development. Further, enhancing NO control capability and auxin supply can significantly increase plant fertility under stress conditions, suggesting that maternal NO homeostasis and auxin supply are key to regulating FG development. Our findings indicate that the maternal plant may integrate internal growth cues (auxin) and external stress intensity (experienced as disrupted NO homeostasis) to determine the success of FG development, providing a mechanism by which plants modulate seed set in response to a fluctuating environment.

Next steps: It is of interest to determine how specific changes in NO modification of proteins contribute to reducing FG development. It is also important to explore the relationship of NO homeostasis to fertility in crop species, with a focus on uncovering the potential application of these molecular mechanisms for crop improvement, particularly in the face of challenging environmental conditions.

sporophytic hypodermal cell in the ovule and develops into a haploid functional megaspore through meiosis (Schneitz et al. 1995; Yang et al. 2010). The functional megaspore then undergoes 3 rounds of mitosis to form the mature FG composed of 7 cells: 3 proximal antipodal cells, 1 central cell, 1 distal egg cell, and 2 synergids (Mansfield et al. 1991; Drews and Yadegari 2002). Proper formation of these cells is necessary for fertilization and zygote development (Ju et al. 2021; Yu et al. 2021).

FG development is closely controlled by the surrounding maternal tissue (Lu and Magnani 2018) that supplies the necessary nutrients as well as space for FG growth upon death of the surrounding nucellar cells (Bajon et al. 1999; Wang et al. 2021a; Yang et al. 1999). In addition, maternal auxin supply is required for FG development, suggesting that maternal control of auxin is key to normal FG development (Wang et al. 2021a). However, what internal signals or how environmental stresses mediate this maternal control of auxin is unknown.

In plants and other organisms, nitric oxide (NO) is dramatically induced by a range of environmental stresses (Fancy et al. 2017), and NO plays a special role in regulating plant growth and development in adapting to adverse environments (Yu et al. 2014; Domingos et al. 2015; Mishra et al. 2021). NO transport, storage, and delivery occur mainly in the form of S-nitrosoglutathione (GSNO; Corpas et al. 2013). The conserved enzyme S-nitrosoglutathione reductase (GSNOR), which functions in GSNO catabolism, thereby plays a central role in modulating NO homeostasis in cells (Frungillo

et al. 2014). In Arabidopsis (*Arabidopsis thaliana*), null mutations of *GSNOR1*, *gsnor1/sensitive to hot temperatures5* (*hot5*)/*paraquat resistant2* (*par2*), show an elevated level of NO species (Feechan et al. 2005; Lee et al. 2008; Chen et al. 2009) and a severe fertility defect that is attributed in part to shorter anther filaments (Lee et al. 2008; Shi et al. 2015). However, how elevated NO contributes to the sterility of *GSNOR* null mutants (hereafter referred to as *hot5* mutants) and what defects beyond filament length are involved have not been elucidated.

We report that GSNOR plays a critical role in maintaining maternal NO homeostasis, which is key to normal FG development, under both optimal and stress conditions. Disrupted maternal NO homeostasis in hot5 mutants or the addition of exogenous NO inhibits the maternal auxin supply to the FG, thereby impacting FG development. Increasing the auxin supply can partially reverse the inhibitory effect on FG development of hot5 mutation or of NO addition. Importantly, enhancing NO control capability and auxin supply can significantly increase plant fertility under salt and drought stresses, suggesting that maternal NO homeostasis and auxin supply are key to regulating FG development. These findings indicate that the maternal plant may integrate internal growth cues (auxin) and external stress intensity (potentially experienced as disrupted NO homeostasis) to determine the success of FG development, providing a mechanism by which plants can modulate seed set under dynamic environments.

Results

The severe sterility of hot5 mutants results from female defects

Mutants of A. thaliana GSNOR, hot5-2 (Columbia [Col]) and hot5-4 (Wassilewskija [WS]), show significantly reduced production of fertile siliques (Lee et al. 2008; Fig. 1, A and B; Supplementary Data Set 1). The short filaments of hot5 mutants have been proposed to prevent pollen delivery to the stigma and to contribute to the sterility (Lee et al. 2008; Shi et al. 2015; Supplementary Fig. S1, A and B). However, we found that most flowers of hot5 plants could produce seeds after manual pollination (Fig. 1C; Supplementary Data Set 2), but that less than 50% of ovules in each silique successfully produced seeds on hot5 plants even with excess pollen (Fig. 1, D and E, and Table 1; Supplementary Data Set 3), indicating that hot5 plants have another fertility defect in addition to short filaments.

Reciprocal crosses demonstrated that the fertility defect was observed only when *hot5* was the female parent (Table 1), and

pollen germination of the hot5-2 mutant was similar to wildtype (WT) germination in an in vitro assay (Supplementary Fig. S1, C and D), suggesting the seed set defect in hot5 mutants results from the female parent.

FG development and nucellus degeneration are delayed in *hot5* ovules

To define the defects in *hot5* ovules that resulted in reduced seed set, we followed pollen tube growth and entry into ovules by aniline blue staining. After manual pollination with self-pollen, more than 90% of WT ovules accepted a pollen tube, while only approximately 50% of *hot5* ovules accepted pollen tubes (Fig. 2A; Supplementary Fig. S2A and Data Set 4), indicating that pollen tube acceptance is disturbed in *hot5* ovules.

The ovules that failed to accept a pollen tube in the *hot5* mutants typically showed callose accumulation (Fig. 2A), which is considered an indicator of a sterile ovule (Vishnyakova 1991). Therefore, we investigated callose accumulation throughout

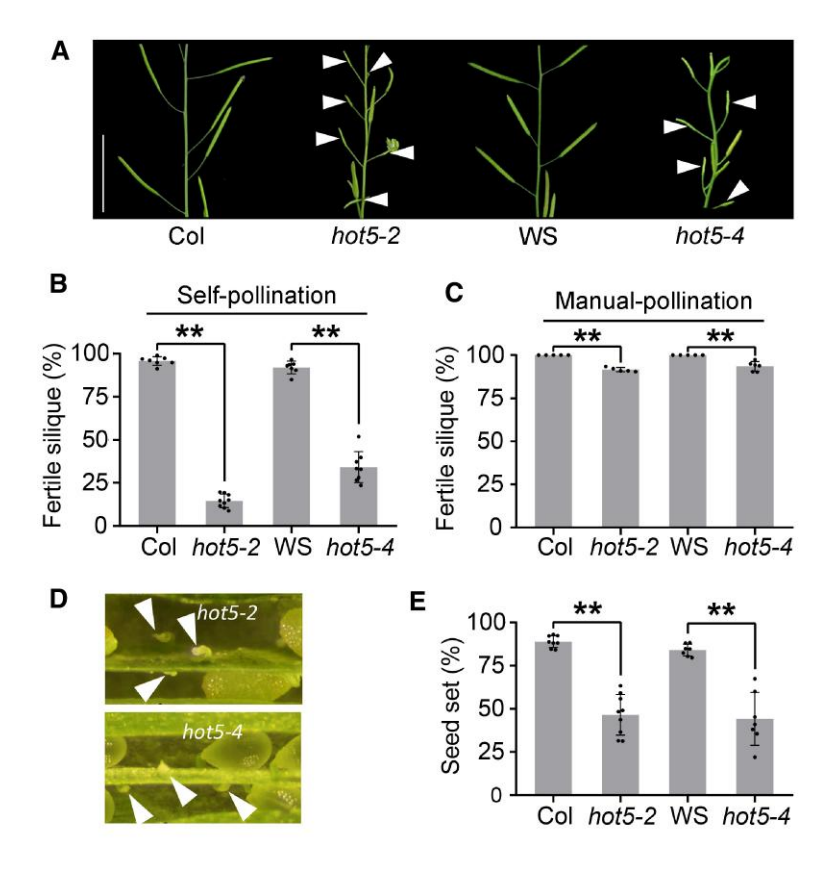


Figure 1. Hot5 null mutants show severe fertility defects. A) Siliques were observed in self-pollinated WT and hot5 mutants, respectively. Arrowheads indicate aborted siliques. Bar = 2 cm. B) The percentage of fertile siliques in self-pollinated WT and hot5 mutants. One dot indicates the average percentage of fertile siliques from 1 plant. Any seed-containing silique was counted as a fertile silique, even if only partially filled. Error bars indicate mean \pm so $(n \ge 7)$. Two-tailed Student's t tests (**P < 0.01). C) The percentage of fertile siliques in WT and hot5 mutants after manual pollination with self-pollen. One dot indicates the average percentage of fertile siliques from 1 plant, and all siliques from each plant were examined. Error bars indicate mean \pm so $(n \ge 5)$. Two-tailed Student's t tests (**P < 0.01). D) Sterile ovules in hot5 mutants. Arrowheads indicate aborted ovules. E) Percent of seed set in each silique after manual pollination in WT and hot5 mutants with self-pollen. Three individual replicates with at least 50 siliques from 7 plants were checked. One dot indicates the percent average seed set from 1 plant. Error bars indicate mean \pm so $(n \ge 7)$. Two-tailed Student's t tests (**P < 0.01).

Table 1. Results of reciprocal crosses

Female × male	Seeds/silique (n)	Ovules/silique (n)	Average seed set (%)
Col x Col	$50.1 \pm 4.3 (12)$	$56.5 \pm 4.1 (20)$	89
$Col \times hot 5-2$	51.2 ± 4.7 (10)		92
$hot5-2 \times Col$	$25.3 \pm 10.8 (12)$	$54.0 \pm 3.7 (20)$	47**
$hot5-2 \times hot5-2$	21.9 ± 9.4 (23)		41**
$WS \times WS$	$40.3 \pm 4.4 (9)$	48.1 ± 4.1 (10)	84
WS \times hot5-4	$39.7 \pm 5.5 (6)$		83
hot5-4 × WS	16.7 ± 11.0 (11)	43.6 ± 1.9 (10)	38**
hot5-4 × hot5-4	17.5 ± 8.7 (8)		40**

n refers to the number of siliques sampled. Two-tailed Student's t tests (**P < 0.01). Pollination was performed 24 HAE of flowers at FDS12, and average percentage of seed set was calculated 7 d after pollination.

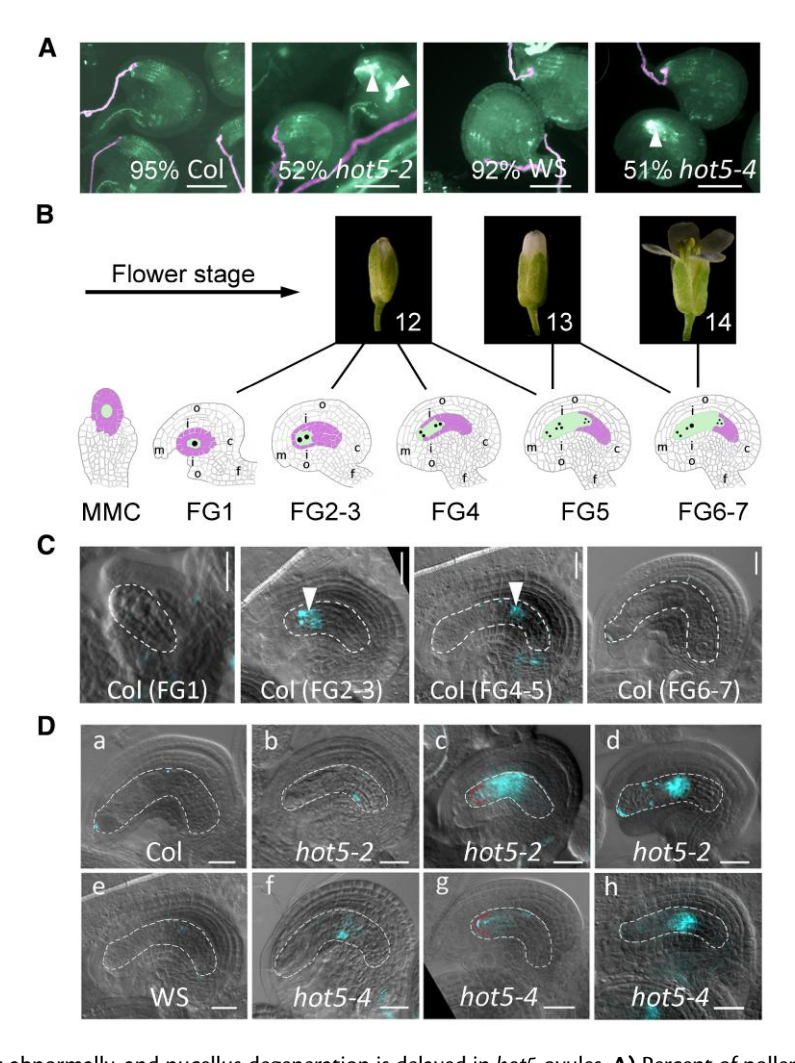


Figure 2. Callose accumulates abnormally, and nucellus degeneration is delayed in *hot5* ovules. **A)** Percent of pollen tubes that enter ovules as assayed by aniline blue staining in WT and *hot5* mutants. Three replicates were performed, and at least 7 pistils for each sample were observed (total ovules: 416 in Col, 725 in *hot5-2*, 328 in WS, and 617 in *hot5-4*). Pollen tubes are false-colored purple. Arrowheads indicate callose accumulation in *hot5* ovules. Bar = 50 μm. **B)** Diagram of WT flowers at FDS12 to FDS14 and corresponding FG developmental stages. m, micropyle; ii, inner integuments; oi, outer integuments; c, chalaza; f, funiculus; MMC, megaspore mother cell. Purple: nucellar cells. Light green: FG region. Black dots: nuclei of the FG. Numbers represent specific developmental stages as previously defined (Smyth et al. 1990; Christensen et al. 1997). **C)** Ovule development and callose deposits in Col ovules. Observations were performed 3 times. At least 3 pistils from flowers at FDS12, FDS13, or FDS14 were sampled each time. Arrowheads indicate callose deposits. Dashed lines outline the developing FG and nucellus region. Bar = 20 μm. **D)** Ovule development and callose deposits in WT (a, e) and *hot5* mutants (b to d, f to h) at FDS14. Compared to WT, *hot5* ovules accumulate callose in the nucellus and show asynchronous ovule development (d, h), and *hot5* even shows extreme defects with nondegenerated nucellar cells at the micropylar end (red dashed lines; c, g). Observations were performed 3 times with 3 plants for each observation, and 2 to 3 pistils were investigated in each plant. White dashed lines outline the developing FG and nucellus region. Bar = 20 μm.

ovule development (stages diagrammed in Fig. 2B). In WT, callose mostly accumulated in the degenerating nucellus of ovules around stages FG2 to FG5 during flower development stages (FDS) 12 to 13 but was occasionally seen in ovules at FDS14, when the ovules are at stages FG6 and FG7 (Fig. 2C). In contrast, hot5 ovules showed intense callose staining and abnormal positioning of callose accumulation at FDS14 (Fig. 2D; Supplementary Fig. S2B and Data Set 5). Consistently, some ovules remained in early developmental stages in hot5 FDS14 flowers, with undegenerated nucellar cells at the micropylar end (Fig. 2, D-c and D-g), which is a characteristic of ovules before FG4. These observations indicated that along with delayed nucellus degeneration, FG development may be retarded in hot5 mutants.

To examine more specific defects in FG development, we introduced 5 FG cell identity promoter:GFP markers (Steffen et al. 2007) into the hot5-2 mutant. Markers of antipodal cells (DD1 and DD6) and synergids (DD11), which are typically expressed from FG4 to FG5, were visible in 10% fewer ovules of the hot5-2 mutant compared to WT at FDS14 (Fig. 3A; Supplementary Data Set 6). In addition, part of the antipodal cell marker in the hot5-2 mutant was positioned relatively closer to the micropylar side (Fig. 3A). Notably, the egg cell (DD45) and central cell (DD22) markers, which are normally expressed starting at FG6, were seen in only about half of hot5-2 compared to WT ovules (Fig. 3A; Supplementary Data Set 6), which is consistent with the reduced hot5-2 seed set. Considering that the egg cell and central cell are necessary for double fertilization (Márton et al. 2005; Chen et al. 2007; Okuda et al. 2009), this result implies that defective FG development contributes to the hot5 sterility.

Confocal laser scanning microscopy (CLSM) observations showed only 64% ovules reached FG6 and FG7 in FDS14 flowers of the *hot5-2* mutant compared to 94% of ovules at FG6 and FG7 in WT (Fig. 3, B and C; Supplementary Data Set 7). Furthermore, delayed pollination experiments showed that the seed set of *hot5-2* was significantly improved at 48 h after emasculation (HAE) compared to at 24 HAE, while there was no significant change in WT seed set (Supplementary Fig. S3 and Data Set 8). These results support that FG development is asynchronous and delayed in the *hot5-2* mutant.

GSNOR protein is absent in the developing FG

To better understand how GSNOR acts in FG development, GSNOR localization in ovules of pGSNOR:GSNOR-GFP transgenic lines was observed in the WT and hot5-2 background, respectively. In pGSNOR:GSNOR-GFP complemented lines, GSNOR-GFP can be visualized in all cells at the ovule primordium stage, including the archesporial cell (Fig. 4, A-a to A-c). However, once the megaspore mother cell undergoes meiosis, developing to FG1, GSNOR-GFP is specifically observed in maternal sporophytic tissues and degenerating megaspores, but absent from the functional megaspore (Fig. 4, A-d to A-f). From this stage on, GSNOR-GFP is not detected

in FG cells throughout FG2 to FG7, but exclusively expressed in maternal sporophytic tissues (Fig. 4, A-g to A-p; Supplementary Videos S1 to S4). Similarly, pGSNOR:GSNOR-GFP in the WT background also showed no detectable protein expression in the FG (Supplementary Fig. S4). Notably, GSNOR-GFP can be visualized in the egg and central cell after fertilization (Fig. 4, B and C), as well as in the zygote and endosperm nuclei (Supplementary Fig. S5 and Videos S5 to S8), highlighting that GSNOR protein is specifically absent from the developing FG until fertilization.

We also evaluated the presence of GSNOR mRNA in the FG by in situ hybridization. GSNOR transcripts are present in nucellar cells at both early and late developmental stages, with weaker expression observed in the FG (Supplementary Fig. S6). Coupled with our observations of GSNOR-GFP expression (Fig. 4), these data suggest that GSNOR protein is not stable or not accumulated in the FG until fertilization, implying that GSNOR activity does not participate directly in FG development, but rather through impact on NO homeostasis in the sporophytic tissues where the protein is clearly present.

Nucellar NO homeostasis is critical to normal FG development

Because the key role of GSNOR is in GSNO catabolism, thereby controlling NO homeostasis (Lee et al. 2008; Frungillo et al. 2014; Shi et al. 2015), we hypothesized that accumulation of NO species would be increased in *hot5* ovules and may contribute to the retarded FG development. 4-Amino-5-methylamino-2',7'-difluororescein diacetate (DAF-FM DA) staining of NO species (Arnaud et al. 2006; Duan et al. 2020) showed a clearer NO-dependent fluorescence signal in *hot5* compared to in WT ovules (Fig. 5A), indicating that more NO accumulates when GSNOR is absent. Specifically, NO species accumulated in the degenerating nucellar cells, which directly contact the FG during FG2 to FG7 (Fig. 5A), highlighting that GSNOR modulates NO homeostasis in maternal tissues.

To determine whether excess NO inhibits FG development, flowers at FDS12a (Christensen et al. 1997) were treated with the exogenous NO donors sodium nitroprusside (SNP) or S-nitroso-N-acetyl-D,L-penicillamine (SNAP). Treated WT flowers showed a significant percentage of ovules (36% or 45%) was delayed before FG6 (mainly at FG5; Fig. 5B; Supplementary Data Set 9), indicating exogenous NO disrupts FG development. In the hot5-2 mutant, delayed FG development was more prominent with SNP or SNAP treatment (Fig. 5B; Supplementary Data Set 9). In contrast, applying the NO scavenger 2-(4-carboxyphenyl)-4,4,5,5tetramethylimidazoline-1-oxyl-3-oxide (cPTIO) significantly reduced the percentage of delayed FGs in the hot5-2 mutant but not in the WT (Fig. 5B; Supplementary Data Set 9), supporting that disrupted NO homeostasis in hot5-2 ovules contributes to delayed FG development.

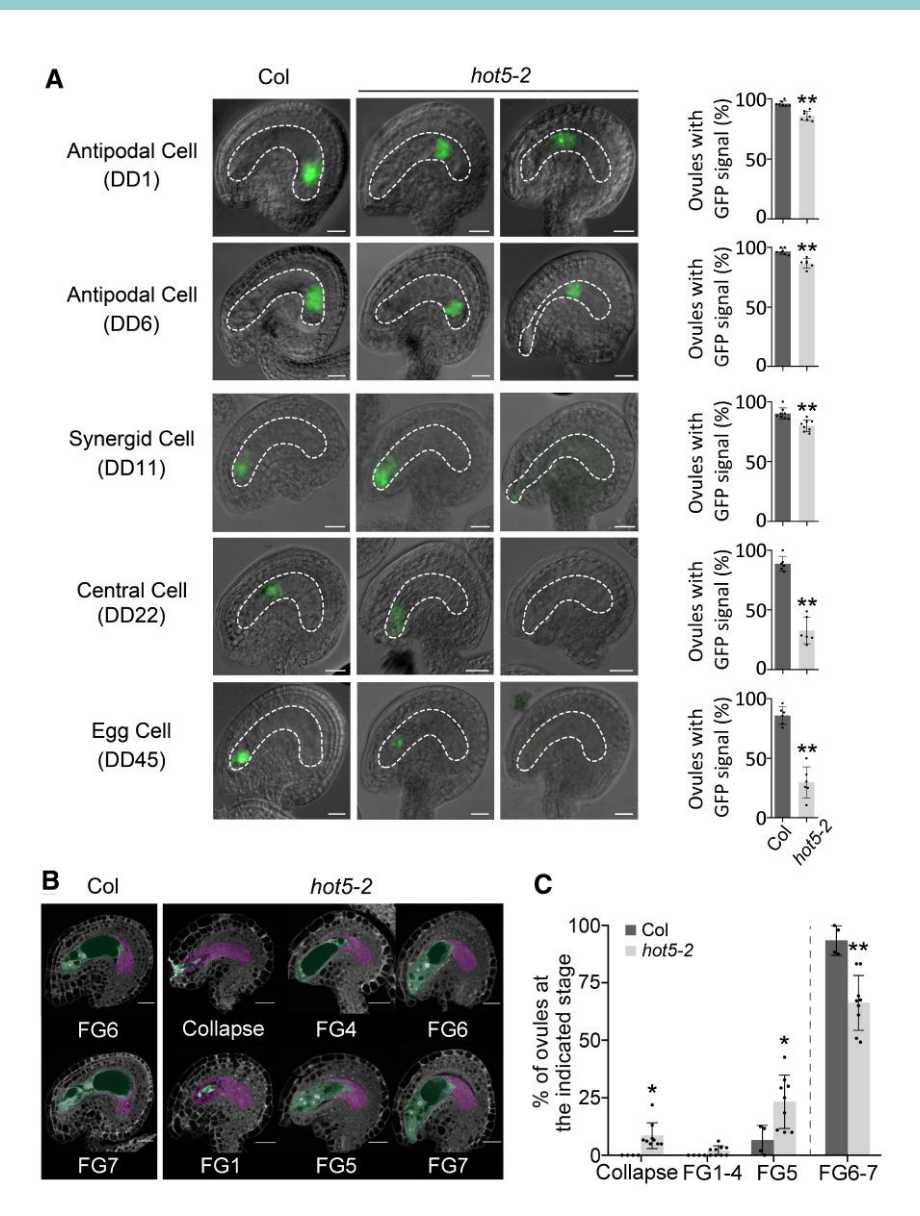


Figure 3. Development of the FG is delayed in a percentage of hot5 ovules. A) The indicated promoter: GFP FG markers (Steffen et al. 2007) in either Col or hot5-2 were observed in ovules from flowers at FDS14. The first and second columns of hot5-2 are samples that show normal and abnormal marker signals in ovules, respectively. The proportion of marker visible at FDS14 is quantified on the right. Observations were performed 3 times, and each dot indicates the average percentage from 1 plant. White dashed lines outline the FG and nucellus region. Fluorescence images are overlaid on differential interference contrast (DIC) images. Bar = 20 μ m. Error bars indicate mean \pm so (n = 6 to 8). Two-tailed Student's t tests (**P < 0.01). B) Ovule development in Col and hot5-2 flowers at FDS14. FG and nucellus are false-colored green and purple, respectively. In hot5-2, FG development is delayed, and a percentage of the FGs are collapsed. Bar = 20 μ m. C) Statistical analysis of FG developmental stage as shown in B). Three replicates with a total of 247 ovules from 9 Col plants and 441 ovules from 15 hot5-2 plants were observed. Each dot indicates a percent of ovules at the indicated FG stage from 2 to 3 plants. Ovules at FG6 and older are mature enough to attract pollen tubes (dotted line). Error bars indicate mean \pm so. Two-tailed Student's t tests (**P < 0.01).

Maternal NO homeostasis indirectly controls FG development

Genetic analysis showed that heterozygous *hot5-2* plants set the same percentage of seeds as WT plants, and *hot5-2* homozygous mutants comprised close to 25% of F₂ plants resulting from self-pollination of a *hot5-2* heterozygote (Table 2). The transmission efficiency of the *hot5* allele was further examined, and it was found that the recovery

of heterozygotes was approximately 50% from reciprocal crosses between $hot5-2~(\pm)$ and Col plants (Table 2). Thus, GSNOR functions in the sporophyte to influence FG development by maternal dominance.

To examine further the maternal-dominant effect of GSNOR in the nucellus, GSNOR-GFP genes were designed to be expressed in the nucellus of hot5-2 driven by the promoter of SPOROCYTELESS (SPL; Yang et al. 1999) and TRANSPARENT

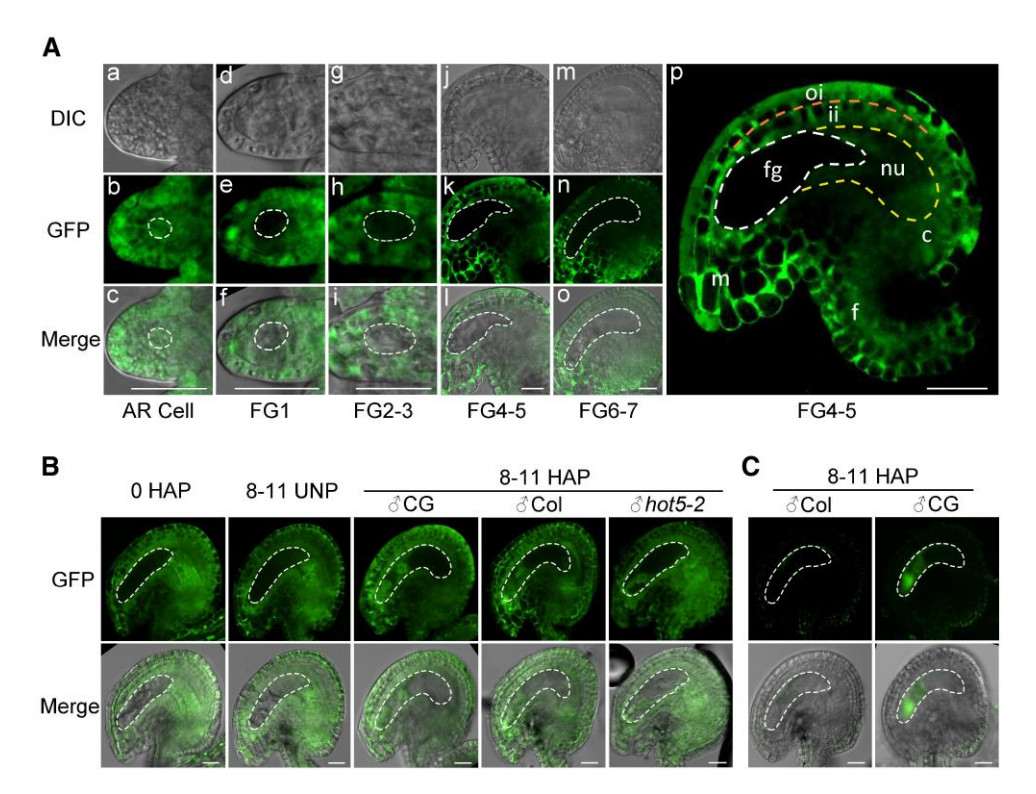


Figure 4. GSNOR-GFP is expressed in maternal sporophytic tissues of the ovule before fertilization and only observed in the FG after fertilization. A) Localization of GSNOR-GFP fluorescence in developing ovules of pGSNOR:GSNOR-GFP complemented hot5-2 (CG) lines before fertilization. (a, d, g, j, m) DIC images showing different ovule stages as indicated. (b, e, h, k, n) Fluorescence images showing GSNOR-GFP signal. (c, f, i, l, o) Merged fluorescence and DIC images at a single Z-plane. (p) Enlarged version of the ovule in (k). White dashed line denotes the FG, yellow dashed line denotes the border between the nucellus and other maternal tissues, and orange dashed line denotes the border between the outer and inner integuments. f, funiculus; c, chalaza; m, micropyle; ii, inner integuments; oi, outer integuments; nu, nucellus; fg, female gametophyte; AR Cell, archesporial cell stage. Bars = 20 μ m (see Supplementary Videos S1 to S4 for additional data). B) Localization of GSNOR-GFP fluorescence in CG lines after fertilization. CG lines were used as the female parent with CG, Col, or hot5-2 lines as the male parent, as indicated. Two independent CG lines were used for this study. Three replicates were performed, with a minimum of 7 pistils observed for each sample in each replicate. White dashed line denotes the FG. HAP, hours after pollination; UNP, hours without pollination, which serves as a control corresponding to the time after ovules were pollinated. Bar = 20μ m (see Supplementary Videos S5 and S6 for additional data). C) Localization of GSNOR-GFP fluorescence in the Col background after fertilization. Three replicates were performed, with a minimum of 7 pistils observed for each sample in each replicate. Col as the female and CG line as the male parent, as indicated. Bar = 20μ m (see Supplementary Videos S7 and S8 for additional data).

TESTA16 (TT16; Xu et al. 2016). As controls, the promoters of EMBRYO SAC-SPECIFIC EXPRESSION1 (ES1; Yu et al. 2005), REDUCED EXPRESSION IN dif1 OVULES6 (DD6), and Reduced Expression in dif1 Ovules45 (DD45; Steffen et al. 2007) were used to drive GSNOR-GFP expression in the FG, antipodal cells, and the egg cell, respectively. As expected, pSPL:GSNOR-GFP (pSPL) and pTT16:GSNOR-GFP (pTT16) constructs were expressed in the nucellus, while pES1:GSNOR-GFP (pES1), pDD6:GSNOR-GFP (pDD6), and pDD45:GSNOR-GFP (pDD45) constructs strongly expressed GSNOR in the FG, antipodal cells, and the egg cell, respectively (Fig. 6A).

All transgenic lines driven by these different promoters showed no significant alterations in plant structure compared to *hot5-2* (Fig. 6B), having enhanced branching. We employed reverse transcription quantitative PCR (RT-qPCR) to determine if the expression of FG markers *DD6*, *DD11*, *DD22*, and

DD45, which show significant downregulation in hot5-2 pistils compared to in Col pistils, is altered in the transgenics (Supplementary Fig. S7). FG marker gene expression in pistils of pES1 transgenics was similar to that in hot5-2 pistils, while in pSPL transgenics, expression recovered to or was higher than that in Col (Supplementary Fig. S7). Notably, plants expressing GSNOR-GFP in the nucellus (in pSPL and pTT16 transgenics) produced longer siliques with higher seed set (Fig. 6, B and C; Supplementary Data Set 10), which was not observed in the pES1, pDD6, and pDD45 plants that expressed GSNOR in the FG. Furthermore, microscopy observations showed that the defects in FG development were rescued only when GSNOR was expressed in the nucellus, not in the FG, antipodal cells, or the egg cell (Fig. 6D; Supplementary Data Set 11). These data support the conclusion that GSNOR and NO are maternal factors regulating plant FG development and that the nucellus is the interface for maternal NO regulation.

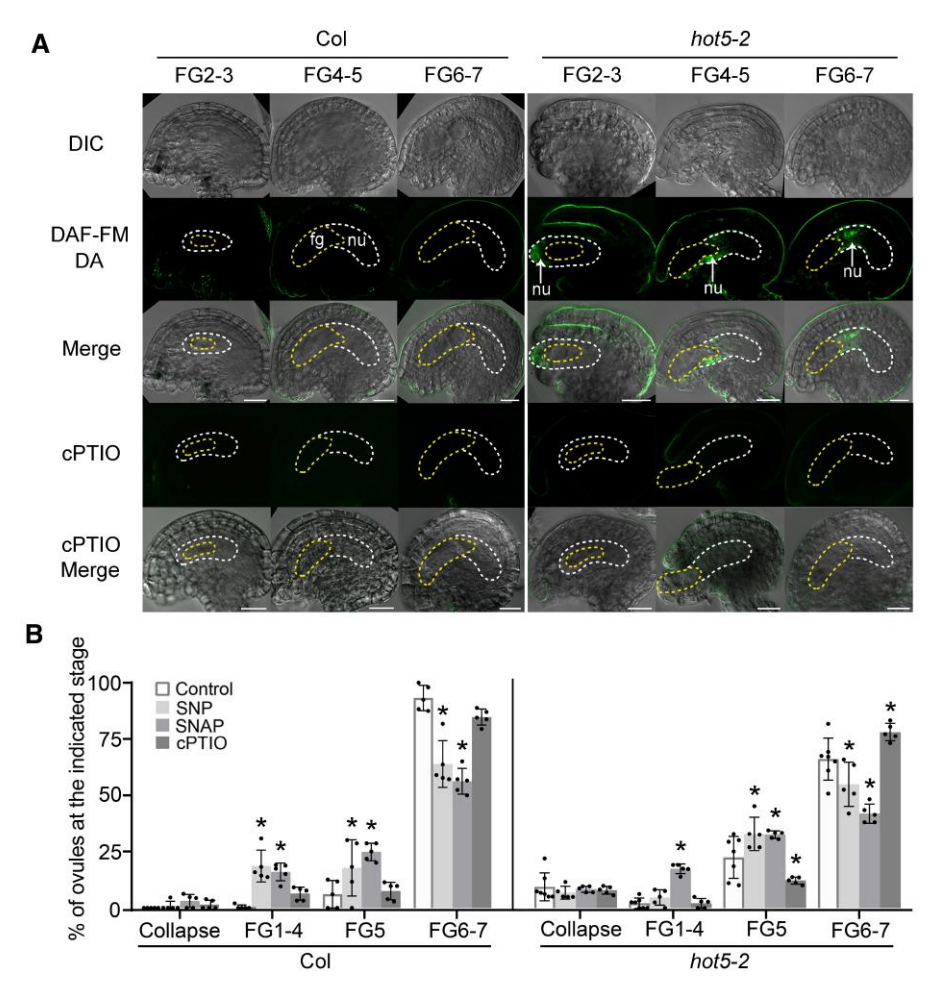


Figure 5. NO homeostasis is critical to normal FG development. **A)** Evaluation of the NO status in ovules of WT and *hot5-2* stained by DAF-FM DA with or without the NO scavenger cPTIO. Yellow dashed line denotes the FG, and white dashed line denotes the border between the nucellus and other maternal tissues. White arrows indicate the location of NO species accumulation in the *hot5-2* nucellus, which is in the process of degenerating based on previous observations (Wang et al. 2021a). fg, female gametophyte; nu, nucellus. Bar = $20 \mu m$. **B)** Statistical analysis of FG developmental stage after SNP or SNAP, or with cPTIO treatment in Col and *hot5-2*. Collapse refers to collapsed FGs with invisible nuclei. Flower buds at FDS12a were treated with the NO donors SNP/SNAP or with the NO scavenger cPTIO and observed by CLSM at FDS14. The number of investigated ovules was 85 for Col, 125 for *hot5-2*, 80 for Col-SNP, 80 for *hot5-2*-SNP, 105 for Col-SNAP, 118 for *hot5-2*-SNAP, 87 for Col-cPTIO, and 99 for *hot5-2*-cPTIO. Each dot indicates the average percentage of ovules at the indicated FG stage from 1 plant. Error bars indicate mean \pm 5D (n = 5 to 7). One-way ANOVA analysis followed by Dunnett's post hoc test (P < 0.05).

Table 2. Transmission rates of hot5 mutant alleles

Genotype	$QCol \times \delta hot 5-2 (\pm) (n)$	$Qhot 5-2 (\pm) \times Col (n)$	Homozygotes in F ₂ population (n)
hot5-2 heterozygote (%)	48.1 (482)	52.9 (353)	24.7 (227)

♀ refers to the female and ♂ refers to the male parent; × refers to the cross. F₂ population comes from the self-pollination of a hot5-2 heterozygote. n refers to the number of plants in the population.

NO homeostasis impacts FG development through the control of maternal auxin transport

Maternal auxin transport is a key mechanism involved in controlling FG development (Wang et al. 2021a). We hypothesized that the FG defects seen in the hot5-2 mutant could be due to altered NO homeostasis affecting maternal auxin supply. To test this hypothesis, transcript levels of

the auxin efflux carriers PIN1 and PIN3, which play a major role in transporting maternal auxin into the developing FG (Wang et al. 2021a), were quantified by RT-qPCR. Compared to in Col, both *PIN1* and *PIN3* were significantly downregulated in pistils of *hot5-2* and SNP-treated Col (Supplementary Fig. S8). Further investigation was performed by examining *pPIN1: PIN1-GFP* and *pPIN3:PIN3-GFP* transgenes in the WT and

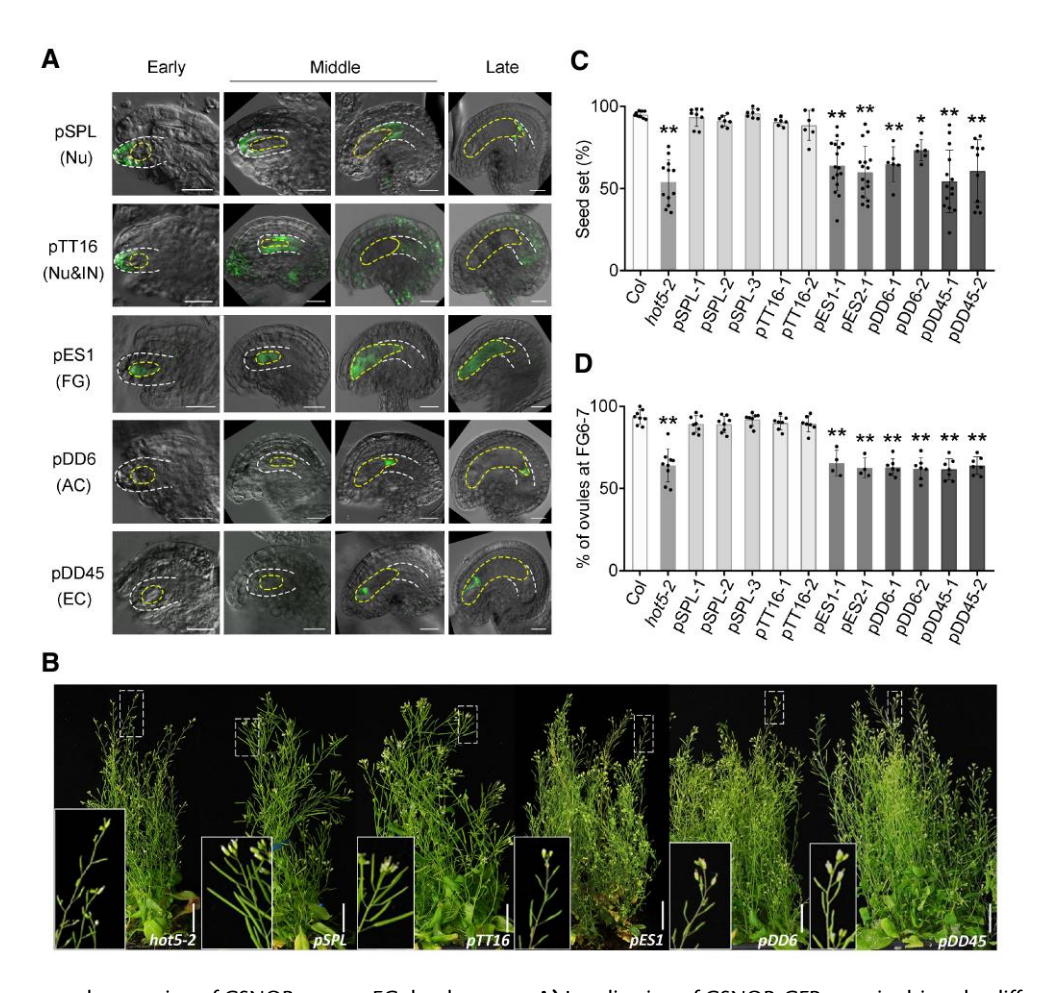


Figure 6. Specific maternal expression of GSNOR rescues FG development. **A)** Localization of GSNOR-GFP protein driven by different promoters in the *hot5*-2 background. *pSPL* is expressed in the nucellus (Nu), *pTT16* is expressed in the nucellus and integuments (Nu&IN), *pES1* is expressed in FG, and *pDD6* and *pDD45* are expressed in the antipodal cells (AC) and egg cell (EC), respectively. Yellow dashed line outlines the FG, and white dashed line denotes the border between nucellus and inner integuments. Early, FG1-2 stage; Middle, FG3-5 stage; Late, FG6-7 stage. Bar = $20 \mu m$. **B)** Phenotype of plants transformed with GSNOR driven by the indicated promoters. Transgenic plants show the *hot5*-2 phenotype of plant structure and flower numbers. The solid white box is an enlargement of the white dotted rectangular region showing the silique phenotype. Bar = 2 cm. **C)** Percentage of seed set in each silique of different transgenic lines. At least 50 siliques from 5 plants were checked per replicate in each line, and 3 replicates were performed. Each dot indicates the average seed set percentage from 1 plant. Error bars indicate mean \pm sp. One-way ANOVA followed by Dunnett's post hoc test (*P < 0.05; **P < 0.01). **D)** Percentage of ovules with FG development at FG6 and FG7 stages in transgenic plants. Each dot indicates the average seed set percentage from 1 plant, and 2 or 3 independent lines were investigated for each transgene. The number of investigated ovules was 166 for Col, 102 for *hot5-2*, 208 for *pSPL-1*, 212 for *pSPL-2*, 215 for *pSPL-3*, 196 for *pTT16-1*, 226 for *pTT16-2*, 135 for *pES1-1*, 139 for *pES1-2*, 191 for *pDD6-1*, 206 for *pDD6-2*, 241 for *pDD45-1*, and 208 for *pDD45-2*. Error bars indicate mean \pm sp. One-way ANOVA followed by Dunnett's post hoc test (*P < 0.05; **P < 0.01).

hot5-2 background. PIN1-GFP was almost undetectable in the hot5-2 nucellus (white arrows in Supplementary Fig. S9A), consistent with the higher accumulation of NO species in the mutant. PIN1-GFP is constitutively present in the funiculus, and PIN3-GFP was also obviously visible in the funiculus from the middle stage (FG3-5) in WT ovules (yellow arrows in Supplementary Fig. S9A). In contrast, both PIN1-GFP and PIN3-GFP were significantly decreased in hot5-2 ovules (Supplementary Fig. S9, B and C, and Data Sets 12 and 13). Furthermore, the application of SNP reduced the level of PIN1-GFP and PIN3-GFP in WT (Supplementary Fig. S9), implying that auxin transport from maternal tissues to the developing FG is suppressed by increased NO. Consistently, the auxin

response, as monitored with DR5::GFP, was decreased in *hot5-2* developing ovules and in SNP-treated WT ovules (Fig. 7, A and B; Supplementary Data Set 14), supporting the conclusion that maternal auxin transport is inhibited by the accumulated NO species.

Auxin levels in the FG were further investigated by using the auxin reporter R2D2, which carries DII-Venus and mDII-tdTomato (Liao et al. 2015). With this semiquantitative reporter, the absence of DII-Venus fluorescence marks auxin accumulation, and mDII-tdTomato provides an internal reference for reporter expression, which allows for ratiometric analysis of relative auxin levels (Fig. 7C). In *hot5-2* or when WT was treated with SNP, auxin levels were significantly

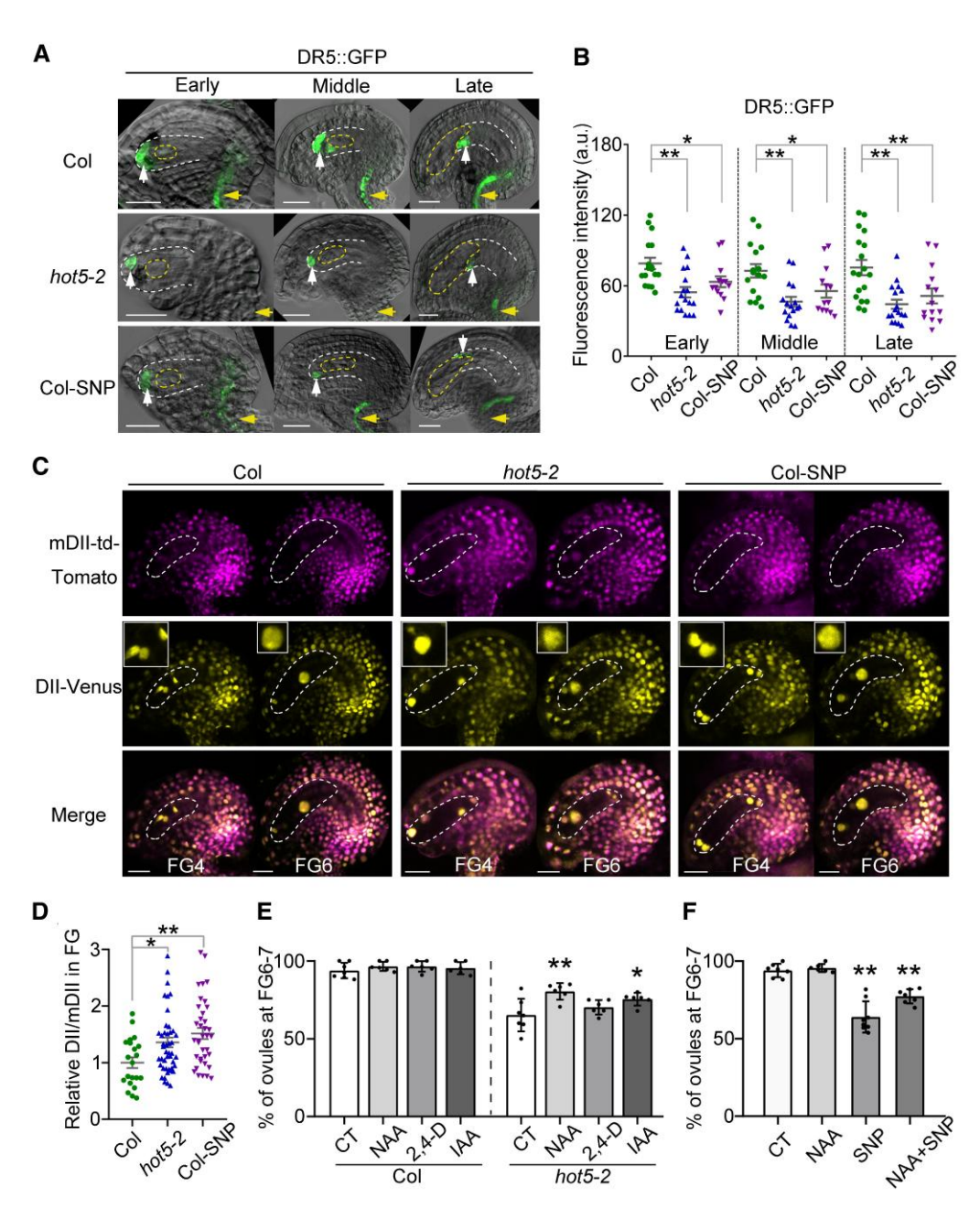


Figure 7. NO accumulation suppresses auxin flow to the FG. A) Auxin response was visualized with DR5::GFP (green) in the developing ovules. White and yellow arrows indicate the nucellus (surrounding the FG) and funiculus, respectively. Bar = $20 \, \mu m$. B) Quantification of fluorescence intensity of DR5::GFP as shown in A). Data from 3 independent experiments. Each value represents the average fluorescence intensity of the entire ovule. Error bars indicate mean \pm SEM ($n \ge 12$). One-way ANOVA with Dunnett's post hoc test (*P < 0.05; **P < 0.01). C) R2D2 expression in Col, hot5-2, and SNP-treated Col ovules during FG development. Magenta for mDII-tdTomato and yellow for DII-Venus. The solid white rectangular box is a 2-fold enlargement of the nucleus in the FG, which shows a stronger DII-Venus fluorescence in hot5-2 and SNP-treated Col. Bars = 20 \(\mu \)m. Micrographs are representative of the typical phenotype of all samples. D) Quantification of relative fluorescent signals of R2D2 (DII/mDII) in the FG. Signal intensity of all visible nuclei in FGs were observed and used to calculate the average value of the DII/mDII ratio. Error bars indicate mean \pm SEM of 3 biological replicates ($n \ge 9$). One-way ANOVA with Dunnett's post hoc test (*P < 0.05; **P < 0.01). **E)** Percent of ovules at FG6 and FG7 after NAA, 2,4-D, or IAA treatment in Col and hot5-2. Data from 3 independent experiments. Each dot indicates the percent of ovules at FG6 and FG7 from 1 plant (total ovule number: 141 in Col, 157 in Col-NAA, 127 in Col-2,4-D, 138 in Col-IAA, 132 in hot5-2, 146 in hot5-2-NAA, 127 in hot5-2-2,4-D, and 119 in hot5-2-IAA). Flower buds at FDS12a were treated and observed at FDS14 by CLSM. Error bars indicate mean ± sp $(n \ge 6)$. One-way ANOVA with Dunnett's post hoc test (*P < 0.05; **P < 0.01). F) Percent of ovules at FG6 and FG7 after NAA, SNP, or NAA + SNP treatment in Col. Data from 3 independent experiments. Numbers of investigated ovules of control, after NAA, SNP, and NAA + SNP treatments were 141, 157, 139, and 147, respectively. Error bars indicate mean ± sD (n ≥ 6). One-way ANOVA with Dunnett's post hoc test (*P < 0.05; **P < 0.01).

reduced in the FG (Fig. 7, C and D; Supplementary Data Set 15). Consistently, the pattern of auxin activity inferred from the R2D2 data was complementary to the pattern displayed by DR5::GFP (Fig. 7, A and B), supporting that disrupted NO homeostasis restricts the maternal auxin supply required for FG development.

To further test the interaction of NO and auxin, we treated flowers from FDS12a with exogenous NAA (exclusively an auxin efflux substrate), IAA, and 2,4-D (exclusively an auxin influx substrate). Only NAA and IAA, but not 2,4-D, significantly reduced the proportion of delayed FGs in the hot5-2 mutant (Fig. 7E; Supplementary Data Set 16), indicating that decreased auxin efflux contributes to delayed FG development, which is associated with disrupted NO homeostasis. Notably, exogenous NAA treatment significantly attenuated the effect of SNP treatment on delaying FG development in WT (Fig. 7F; Supplementary Data Set 17), supporting the conclusion that NO homeostasis and auxin delivery are critical in regulating FG development. Taken together, we propose that maternal NO homeostasis regulates FG developmental processes and ultimately fertility in part through modulating maternal auxin supply.

Enhanced GSNOR expression and auxin supply protect FG development under drought and salt stress

The fact that NO can accumulate under stress conditions (Xie et al. 2013; Shi et al. 2014) suggests that stress could negatively affect fertility due to an impact of NO homeostasis on auxin supply. To test this hypothesis, we subjected A. thaliana to short-term salt and drought stress during flowering in hot5-2 complemented lines that, despite GSNOR being driven by the native promoter, show higher protein expression (Xu et al. 2013) and higher transcript levels (Fig. 8A). Compared to WT, these transgenic overexpression (OE hereafter) lines showed similar fertility and developmental phenotypes (Supplementary Fig. S10). However, under both drought and salt stress, the OE lines showed increased fertility and longer siliques with fewer aborted ovules compared to WT (Fig. 8, B and C; Supplementary Tables S1 and S2).

Under drought stress, imposed for 4 d with 1% or 2% PEG, WT seed set decreased from an average of 93.1% in untreated controls to 73.0% and 63.0%, respectively, while the seed set of OE lines decreased on the order of 10% less, from 93.1% to 83.7% and 75.0%, respectively (Fig. 8D; Supplementary Table S2 and Data Set 18). Similarly, enhanced seed set was observed with 4 d of salt stress at 100 or 200 mm NaCl; while WT seed set decreased to 68.2% and 60.3%, respectively, the OE lines maintained seed set at 78.9% and 72.8%, values that are significantly higher than those in WT (Fig. 8D; Supplementary Table S2). Reciprocal crosses showed that 3 or 5 d of stress significantly depressed both female and male fertility, and that fertility could be enhanced by GSNOR OE (Supplementary Fig. S11 and Data Set 19). Consistently, microscopy observations confirmed that FG

development is significantly faster in OE lines, as a greater percentage of ovules reached FG6 and FG7 under stress in OE lines compared to in WT (Fig. 8E; Supplementary Table S3 and Data Set 20), supporting the idea that enhancing NO control can protect plant fertility under stress conditions.

To examine the potential role of auxin efflux in the stress resistance conferred by GSNOR OE, we applied exogenous NAA and 2,4-D to both WT and an OE line along with the stress treatments. NAA significantly rescued FG development and seed set in WT and further enhanced stress resistance in the GSNOR OE line, while 2,4-D did not (Fig. 8E; Supplementary Fig. S12 and Data Sets 20 and 21). Under drought or salt stress, imposed with 2% PEG or 200 mm NaCl, the addition of NAA improved the FG6-7 percent of WT from an average of 70.1% to 79.6% or from 68.4% to 78.3%, respectively, and improved the FG6-7 percent of OE line from an average of 81.0% to 87.0% or from 78.6% to 86.0%, respectively, while the addition of 2,4-D had no significant effect (Supplementary Table S3). Microscopy observations showed that the addition of NAA also rescued FG development with a greater percentage of FGs reaching FG6 and FG7 under stress, while 2,4-D did not (Fig. 8E; Supplementary Data Set 20). These results provide further support for the role of auxin efflux in FG development under environmental stress.

Together, these data indicate NO homeostasis and auxin delivery are critical to the production of offspring under stress conditions, and that the increased fertility achieved by enhancing GSNOR expression or auxin supply provides an approach to protect FG development during stress.

Discussion

Our data indicate that GSNOR is a maternal factor mediating FG development, acting in part through the impact of NO homeostasis on auxin efflux from the sporophyte to the FG. Restricted auxin efflux associates with retarded FG development that leads to reduced fertility. Our data further suggest that NO homeostasis, which can be disrupted under many stress conditions, is a critical component of the mechanism by which plants respond to their environment to optimally adjust surviving offspring number. In total, NO homeostasis as controlled by GSNOR is essential to normal auxin efflux, normal FG development, and final fertility (Fig. 8F).

Reduced fertility of GSNOR null mutants has previously been noted and ascribed primarily to reduced anther length (Lee et al. 2008; Shi et al. 2015). However, we clearly show that hot5 pollen is fully viable and that delayed and abnormal development of up to 50% of ovules is a major contributor to the hot5 fertility defect (Fig. 1; Supplementary Fig. S1 and Data Sets 1 to 3). Fewer ovules reach the FG6 and FG7 stages synchronized for fertilization, many ovules accumulate callose abnormally (Fig. 2; Supplementary Data Set 5), and production of the central cell and egg cell is delayed or does not occur in many ovules (Fig. 3; Supplementary Data Set 6). We found that GSNOR protein is expressed in maternal tissues and

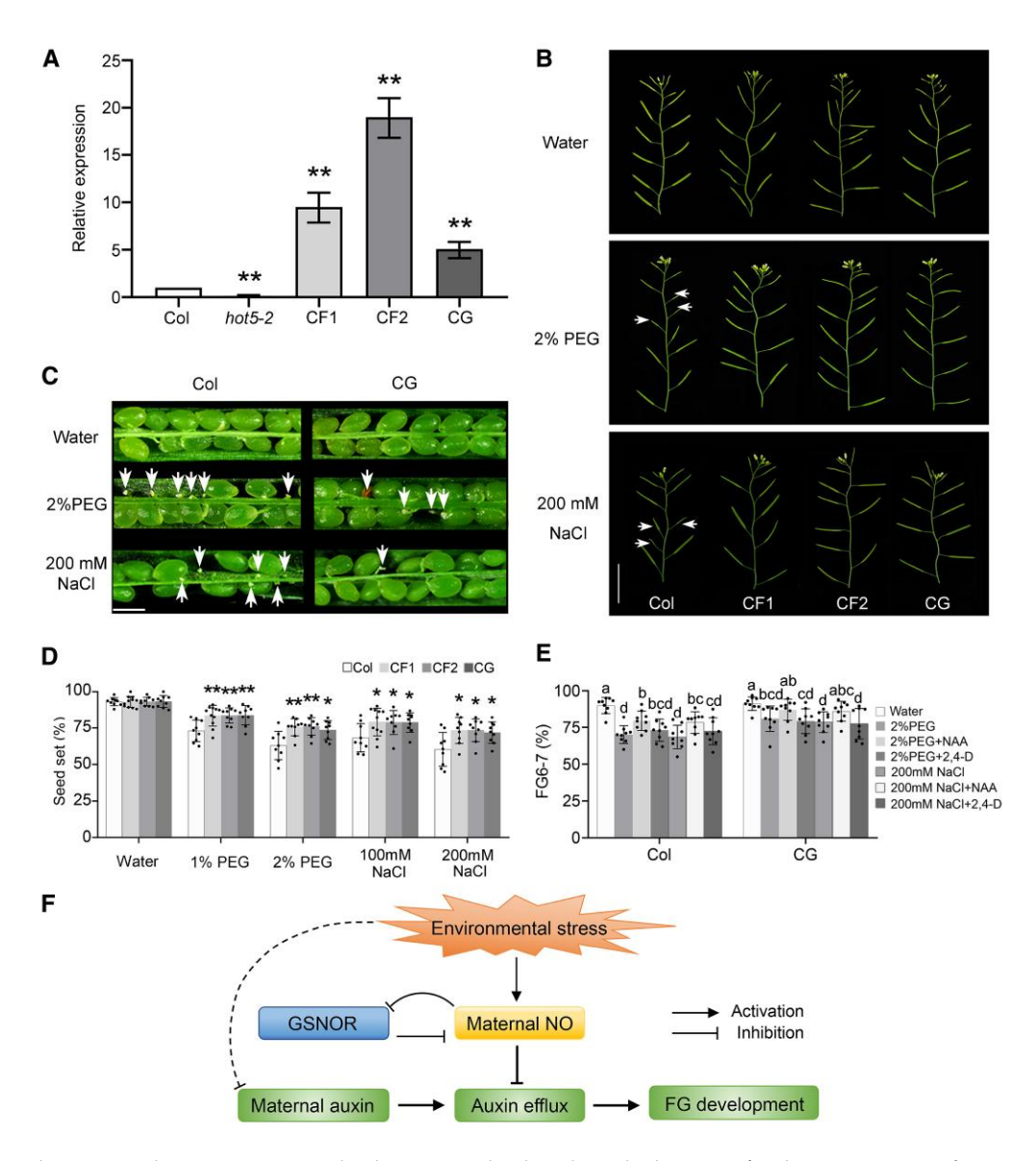


Figure 8. Increased GSNOR and NAA promote FG development under drought and salt stress. **A)** Relative expression of GSNOR in pistils of Col, hot5-2, and 3 independent complemented lines with the WT genomic GSNOR translationally fused to a FLAG tag (CF1 and CF2) or to GFP (CG). RT-qPCR was performed on 3 technical replicates of 3 independent biological replicates. Error bars indicate mean ± sp. One-way ANOVA with Dunnetts post hoc test (**P < 0.01). **B)** Silique development of Col and hot5-2 complemented lines before and after 4 d of the indicated stress and recovery for 3 d. White arrows indicate sterile siliques. The first silique at the bottom was developed from a flower at FDS14 at the time of treatment. Bar = 2 cm. **C)** Seed set of WT Col and complemented lines before and after stress. White arrows indicate aborted ovules. Bar = 500 μm. **D)** Statistical analysis of seed set before and after stress. Seed set was analyzed from flowers that were at FDS12a at the time of treatment and observed at FDS14. Data from 3 independent experiments, and each dot represents 1 plant. Error bars indicate mean ± sp (n ≥ 9). One-way ANOVA with Dunnett's post hoc test (*P < 0.05; **P < 0.01). **E)** Auxin efflux restores FG development under stress. Plants were stressed after bolting for 7 d. During the stress, the inflorescence was treated with NAA (5 μM) or 2,4-D (5 μM) by dipping. Inflorescences were treated every 6 to 8 h for 3 min each time over 4 d. Data from 3 independent experiments, and each dot represents the percent of ovules at the indicated FG stage from 1 plant. Error bars indicate mean ± sp (n = 9). Different letters on graphs indicate significant difference (P < 0.05) calculated by one-way ANOVA followed by Fisher's LSD test. Significant differences (by 2-tailed Student's t tests) were detected between Col and CG under 2% PEG and 200 mL NaCl conditions, but no significant differences were detected between Col and CG under control (water) condition. **F)** Model for how GSNOR modulates maternal NO homeostasis to

not detected in the developing FG until after fertilization (Fig. 4). Although single-cell RNA-seq data indicate that there is little change of GSNOR mRNA levels between the egg cell and the early zygote (Zhao et al. 2019), we found that

GSNOR protein is expressed in the zygote, but not in the developing FG (Fig. 4; Supplementary Fig. S5 and Videos S5 to S8). These data indicate that even though GSNOR mRNA is detected in the FG, it is potentially not accumulated until after

fertilization. Therefore, these dramatic fertility phenotypes can be linked to the disruption of NO homeostasis in maternal tissues when *GSNOR* is mutated. The importance of maternal GSNOR activity is further emphasized by the fact that expressing *GSNOR* specifically in maternal tissues, but not in the FG of the *hot5* null mutant, eliminated the FG developmental delay and restored fertility. These data also demonstrate the importance of considering not only mRNA but also protein levels when assessing developmental controls.

This study used two promoters (SPL and TT16) to test the requirement for GSNOR expression in the maternal plant as opposed to the FG. Although the TT16 promoter may cause premature degradation of the nucellus (Xu et al. 2016), our results showed that both promoters significantly rescued seed set and FG development when used to drive GSNOR expression. There was no significant difference in the rescued effect between the two promoters (Fig. 6, C and D; Supplementary Data Sets 10 and 11), supporting the importance of GSNOR activity in maternal tissues.

The control of NO species and protein nitrosation levels by GSNOR could also be important for the function of the LURE protein, which is needed to attract the pollen tube and which is inactivated by nitrosation (Duan et al. 2020). Indeed, we found that 64% ovules are at the FG6 and FG7 stages in hot5, and only ~50% successfully attracted a pollen tube (Fig. 2), indicating that the defects of the hot5 ovule are complex. The failure of pollen tube attraction to hot5 ovules may result in part from high NO species leading to LURE nitrosation, as well as being a consequence of the delayed FG development seen in hot5 ovules.

Even in the hot5 GSNOR null mutant, NO species as detected by DAF-FM are only obvious in the nucellus and at the ovule surface (Fig. 5A), not in all cells, suggesting that the production of NO is not uniform. The DAF-FM signals detected at the ovule surface were significantly reduced after cPTIO treatment, suggesting NO species accumulate at these locations, which may result from mechanical wounding (Corpas et al. 2011) when ovules are dissected from the pistil. However, NO species at the surface in WT ovules are much lower than in hot5-2 ovules (Fig. 5A), consistent with the role of GSNOR in controlling NO homeostasis. NO may not be produced in the FG, or any NO that is produced may be found conjugated to protein Cys, Tyr, or to metals and be undetectable by DAF-FM (Balcerczyk et al. 2005). However, NO species were readily observed to accumulate in the degenerating nucellus when GSNOR is absent (Fig. 5A). These observations demonstrate that NO metabolism is distinct in different cell types of the ovule, potentially related to different cell functions.

Auxin has broad roles in plant development. It is synthesized in shoot and root apices and transported to positions of new organ initiation (Zhao 2010), potentially guiding the partitioning of plant nutrients for new organ development (Liu and von Wirén 2022). The PIN proteins, which are auxin efflux carriers, play the core role in long-distance auxin transport (Petrasek et al. 2006; Adamowski and Friml 2015) and are essential for

the transport of maternal auxin into the developing FG to maintain FG development (Wang et al. 2021a). Previous work has shown that the expression of the major PIN proteins, PIN1 and PIN3 (Shi et al. 2015; Wang et al. 2021a), is severely suppressed by NO (Meyer et al. 2014; Shi et al. 2015). We found PIN1 and PIN3 expression is reduced in ovules of hot5 and in WT with application of an NO donor (Supplementary Fig. S9), and that expression was associated with decreased auxin activity as revealed by DR5::GFP (Fig. 7, A and B; Supplementary Data Set 14). In addition, the pattern of auxin activity revealed by the ratiometric reporter R2D2 was consistent with that of DR5::GFP. Thus, auxin levels are reduced in the FG when NO homeostasis is dysregulated (Fig. 7, C and D; Supplementary Data Set 15), leading to delayed FG development. However, this delay can be rescued in the hot5-2 mutant by applying an auxin efflux substrate, which emphasizes the critical role that maternal auxin plays in FG development (Wang et al. 2021a). This observation further strengthens the link between NO homeostasis and auxin delivery from maternal tissues to the developing FG. We note, however, that the current data do not allow us to rule out the possibility that NO accumulation may affect auxin biosynthesis or auxin signal transduction.

Because GSNOR functions as a major enzyme in NO catabolism (Gupta et al. 2011; Li et al. 2021), control of its activity is critical to NO homeostasis. GSNOR activity has been demonstrated to decrease under conditions that produce high NO, potentially due to nitrosation of specific Cys residues (Guerra et al. 2016; Zhan et al. 2018). A current model suggests that when subjected to stresses, NO can be produced to levels that partially inhibit GSNOR activity, resulting in a local NO increase (Frungillo et al. 2014; Domingos et al. 2015; Guerra et al. 2016). Therefore, the regulation of GSNOR activity by NO in maternal tissue could function to evaluate the intensity of environmental stresses. We show that manipulating NO homeostasis by increasing GSNOR or adding auxin efflux substrate increased fertility under stress conditions, while NO donors decreased fertility (Fig. 8; Supplementary Data Sets 18 and 20). Increased NO during stress could therefore act to integrate the effects of auxin on new organ initiation and growth (Meyer et al. 2014; Shi et al. 2015), as we show for FG development. We speculate that NO-mediated auxin partitioning is a general mechanism for plant adaptive development under stress.

More and more data show that the development of the FG during flowering is a key stage at which stress causes loss of crop yield (Albertos et al. 2019; Lohani et al. 2020; Wang et al. 2021b). Our results suggest that stress-induced disruption of NO homeostasis delays FG development, providing a mechanism for plants to optimize investment in viable offspring. Importantly, we saw fertility increases on the order of ~10% with enhanced GSNOR expression or increased auxin delivery. Thus, final crop yield under stress may be achieved by better control of NO homeostasis or by increasing available auxin to protect FG development, especially when stress occurs during critical reproductive stages.

Materials and methods

Plant material and growth conditions

hot5-2 and hot5-4 are AtGSNOR (At5g43940) mutants of Arabidopsis (A. thaliana) with a T-DNA insertion in the first exon in the Col background and in the fourth exon of the WS background, respectively (Lee et al. 2008). Transgenic hot5-2 plants complemented with proGSNOR: GSNOR-FLAG or proGSNOR:GSNOR-GFP were constructed as previously described (Xu et al. 2013), and 3 independent lines were used for this study. Transgenic plants carrying GFP driven by promoters of different FG markers, DD1, DD6, DD11, DD22, and DD45, in the Col background (Steffen et al. 2007) were obtained from Ravi Palanivelu (University of Arizona, United States) and were introduced into the hot5-2 background by crossing. Transgenic plants carrying the GSNOR-GFP driven by different ovule marker promoters, proSPL (Yang et al. 1999), proTT16 (Xu et al. 2016), proES1 (Yu et al. 2005), proDD6, and proDD45 (Steffen et al. 2007), were introduced into the hot5-2 background. PINs-GFP and DR5::GFP plants were previously described (Wang et al. 2021a).

Plants were grown in peat with a 16-h light/8-h dark (150 μ mol/m²/s) and a 21/19 °C day/night cycle in a growth chamber as previously described (Xu et al. 2013).

Plasmid construction and plant transformation

The vectors *proGSNOR:GSNOR-FLAG/GFP* were constructed as previously described (Xu et al. 2013). For the constructs carrying the *GSNOR-GFP* gene driven by different ovule marker promoters, the genomic DNA sequences of *SPL* (AT4G27330, 3.9 kb), *TT16* (AT5G23260, 3.4 kb), *ES1* (AT5G40260, 1.5 kb), *DD6* (AT2G42930, 1.1 kb), and *DD45* (AT2G21740, 1.0 kb) were amplified from Col-0, and genomic DNA of *GSNOR* fused with *GFP* at the C-terminus was amplified from the plasmid of *proGSNOR:GSNOR-GFP* construct, then cloned into pCAMBIA 1300s. Construct sequences were verified before being introduced into *Agrobacterium tumefaciens* strain GV3101 to shuttle these binary vectors into plants by the floral dip method (Clough and Bent 1998).

Fertility analysis

The seed set percentage per silique was determined using the 3rd to the 10th flowers, 10 wk after germination. The percentage of fertile siliques on each plant was also measured 10 wk after germination, and any silique with seeds was scored as fertile. Manual pollination was applied according to the following protocol: flowers were emasculated at FDS12a, and 20 to 24 h later, emasculated flowers were pollinated with pollen from flowers at FDS14 (Smyth et al. 1990; Christensen et al. 1997). About 1 wk later, the number of sterile ovules and total ovules were counted to determine the percent of seed set. For reciprocal crosses, 5-wk-old WT and hot5 plants were used. Flowers of WT and hot5 at FDS12a were emasculated, and pistils were then manually pollinated after 20 to 24 h with pollen grains of WT or hot5 plants, reciprocally. For delayed pollination, flowers of

WT and *hot5* at FDS12a were emasculated, and pistils were then manually pollinated after 24, 48, and 72 h with pollen grains of WT or *hot5* plants, reciprocally.

Aniline blue staining and pollen tube germination in vitro

Ovule acceptance of pollen tubes was observed 18 to 24 h after manual pollination by aniline blue staining. Pistils of WT and hot5 were emasculated at FDS12 and then manually pollinated with self-pollen grains at FDS14. Pistils were fixed in 250 μ L of 10% (v/v) acetic acid in ethanol for at least 3 h, and then samples were softened with 1 M NaOH overnight at room temperature. Samples were washed gently 3 times with 50 mm K_3PO_4 buffer (4.17 mL 1 m K_2HPO4 and 0.83 mL 1 m KH_2PO4 , pH = 7.5). Pistils were then stained with 0.01% (w/v) aniline blue (dissolved in 50 mm K₃PO₄ buffer) for at least 2 h, but not more than 12 h in the dark (Duan et al. 2014). The stained samples were transferred to slides, and callose was observed under an Axio Imager M2 fluorescence microscope (Zeiss) equipped with a UV filter set. The pollen germination in vitro was evaluated following the method from Boavida and McCormick (2007).

Chemical treatments

The NO donors SNP and SNAP and the NO scavenger cPTIO were obtained from Sigma (United States) and dissolved in 10 mm phosphate-buffered saline, pH = 7.4 (Lee et al. 2008). Floral buds at FDS12a (Smyth et al. 1990; Christensen et al. 1997) were immersed in a solution of 500 μ M SNP/SNAP or 100 μ M cPTIO, with 0.005% (v/v) Silwet L-77 (Solarbio, China). Samples were treated every 7 h for 2 min and were taken for observation 3 h after the fifth treatment, when the flower was at FDS14. Treatment with a 0.005% (v/v) Silwet L-77 solution served as a negative control. For SNP or SNAP treatment, we tested 100, 500, and 1,000 μ M concentrations; 100 μ M concentration showed no significant inhibition, and 1,000 μ M concentration inhibited flower opening with sepals and petals turning yellowish-brown. Therefore, 500 μM concentration was selected for evaluation. For cPTIO treatment, we tested 10, 100, and 500 μ M concentrations; 10 μ M cPTIO showed no significant effect, and 500 μ M cPTIO inhibited flower opening. Thus, 100 μ M cPTIO was selected for the experiments. The flower buds were treated with 5 μ M NAA, 2,4-D, or IAA at FDS12a. For the SNP + NAA treatment, the mixture of 5 μ M NAA and 300 μ M SNP was used. Samples were treated every 3 to 5 h for 3 min each time and were taken for observation at FDS14. Treatment with a 0.005% (v/v) Silwet L-77 solution served as a negative control.

RT-qPCR analysis

Pistils were sampled from flowers of WT, hot5-2, pES1, pSPL, and pGSNOR:GSNOR complementary lines at FDS14. For each sample, total RNA was extracted from more than 50 pistils according to manual of the total RNA Pure Plant Kit (TIANGEN, China, DP441). Reverse transcription reactions

were then conducted via PrimeScript RT reagent Kit with gDNA Eraser (TaKaRa, Japan, RR047) from $1 \mu g$ of RNA. qPCR reactions for selected candidate genes were performed with the TB Green Premix Ex Tag II (TaKaRa, Japan, RR820) on an Applied Biosystems QuantStudio 3 instrument. The GSNOR primers were (5'-GGGAAGACTAACCTTTGTGG-3') as the forward and (5'-AATTTTGGCGACGCTAACATC-3') as the reverse. The PIN1 primers were (5'-TTACGGCTCTG TCAAATGGT-3') as the forward and (5'-GTTGTTAGCGGC G-ATGAAGT-3') as the reverse. The PIN3 primers were (5'-CCCTCATGGTCCAAATCGTC-3') as the forward and (5'-GCTTCCCGTCGTCACCTATC-3') as the reverse. The DD6 primers were (5'-TTTCAGTAGCAGGAACATCAG-3') as the forward and (5'-AAATCGCAGTTT-CTGGGTAT-3') as the reverse. The DD11 primers were (5'-CCACGAACTCC TAAGCCA-CA-3') as the forward and (5'-CACAACAATCC TCCGAAACG-3') as the reverse. The DD22 primers were (5'-TGCTTATCATATTTGCCACAG-3') as the forward and (5'-GCCCGTC-ACATTTACTTTCG-3') as the reverse. The DD45 primers were (5'-ACAAACATAGCGG-CAAGACT-3') as the forward and (5'-AGATTGACAGAAACCACGAAG-3') as the reverse. ACTIN2 was used as an internal control. Three biological replicates were performed.

RNA in situ hybridization

RNA in situ hybridization was performed in whole-mount ovules as previously described (Hord et al. 2006). Briefly, inflorescences of 6-wk-old WT plants were fixed in FAA (50% [v/v] ethanol, 5% [v/v] acetic acid, and 3.7% [v/v] formaldehyde) at 4 °C for 12 h with vacuum infiltration on ice. The samples were then dehydrated, cleared in dimethylbenzene, and embedded into Paraplast (Sigma, United States). Sections 8 μ m thick were prepared on slides that were dewaxed and treated with $5 \mu g/mL$ proteinase K (Thermo Fisher Scientific) at 37 °C for 30 min. RNA probes labeled with digoxigenin were hybridized to the slides. For RNA probe synthesis, specific cDNA fragments of the GSNOR gene were PCR amplified with primers containing SP6 and T7 promoter sequences. An antisense probe was generated using T7 RNA polymerase, and the sense probe was synthesized using SP6 RNA polymerase. The GSNOR antisense probe used (5'-CCCATTTATCACTTCATGGGTA-3') as the forward and (5'-ACACTAATACGA-CTCACTATAGGGGG GTTCACAAATTCGTTAACAC-3') as the reverse primers. Hybridization and signal detection were performed according to the manual of the DIG RNA labeling kit (Roche; 11175025910). The sections were mounted in 50% (v/v) glycerol and imaged via an Olympus BX53 microscope.

Imaging NO status in A. thaliana ovules

The NO status of ovules was visualized by staining with DAF-FM DA (Thermo Fisher Scientific). The ovules of flowers at FDS14 were dissected quickly to minimize light exposure and then incubated in 30 μ L of 20 μ M DAF-FM DA, which was dissolved in DMSO for stock and diluted to working concentrations in 20 mM HEPES, pH = 7.5, for 15 to 30 min

at 22 °C in the dark, followed by 2 to 3 washes with 20 mm HEPES. Treatment with an identical final DMSO concentration was performed as a negative control. The ovule samples were examined and imaged immediately by CLSM.

Microscopy

For the examination of FG development, CLSM was performed according to the method described by Christensen et al. (1997) and Shi et al. (2005). Pistils at FDS14 from WT and hot5-2 were fixed, dehydrated, cleared, and dissected to observe with an Olympus Fluoview FV1000 confocal laser scanning microscope with a 488-nm argon laser and an LP 530 filter. The GFP signal for the ovule and FG markers was observed with an Olympus fluorescence microscope FV1100 for ovules at FDS12 to FDS15, using Col and hot5-2 carrying no GFP markers as controls for background fluorescence. GSNOR-GFP was observed using the Olympus Fluoview FV1100 and FV1200 confocal microscope, and NO species-related fluorescence after DAF-FM DA staining was observed using a Leica SP8 laser confocal microscope. For observation of GSNOR-GFP after fertilization, hand pollination was used. CG and WT flowers were emasculated at FDS12c (Smyth et al. 1990) and were pollinated after 24 h (Duan et al. 2020). They were either pollinated or left without pollination (as the control). Individual ovules were dissected from the pistils at 8 to 11, 15 to 18, and 22 to 25 h after pollination. For observation of NO species, unstained samples were included as a control. For the R2D2 line, a Zeiss LSM880 was used for imaging. For each observation, blank controls of Col and hot5-2 were used to set the viewing parameters, which were then applied to all samples. The GFP and DAF-FM DA staining was scanned with excitation at 488 nm and detection at 495 to 535 nm. Venus was excited at 514 nm and detected at 524 to 540 nm; tdTomato was excited at 561 nm and detected at 571 to 630 nm. Measurement of nuclear fluorescence intensity of the FG was used to calculate the mDII/DII ratio; measurement of fluorescence intensity of the whole nucellus was used to calculate the mDII/DII ratio. The mDII/DII ratio was calculated as described previously (Liao et al. 2015). ImageJ 1.48V software was used to process the pictures and obtain fluorescence intensity.

Salt and drought stress treatments

Different ecotypes and genotypes of plants were planted in the same pot and grown under normal conditions. Five to seven days after bolting, the plants were subjected to treatments including water (control), 100 or 200 mm NaCl, or 1% (w/v) or 2% (w/v) PEG for a duration of 4 d. Flowers at FDS14 were labeled at the end of treatments and were investigated for seed set after normal watering for 7 d. After watering with 100 mm NaCl and 1% (w/v) PEG, only a minor change of seed set was observed in WT; thus, we chose 200 mm NaCl and 2% (w/v) PEG for subsequent stress treatments. All pots were rotated daily during the treatments to minimize chamber effects. During the stress treatments, the inflorescence of WT (Col) or GSNOR OE (CG) plants was treated with NAA (5 μ m) or 2,4-D (5 μ m) by dipping.

Samples were treated every 6 to 8 h for 3 min each time and were harvested for FG developmental observations at FDS14 at the end of the treatments. Seed set was investigated after recovery for 7 d as noted above. For reciprocal crosses, flowers at FDS12a of stressed plants or control plants were emasculated and then manually pollinated after 20 to 24 h. Reciprocal crosses were performed between control plants and stressed plants of the same genotype, and control WT × control WT was a technical control. Reciprocal crosses were performed when the plants were stressed for 1, 3, and 5 d, respectively. After treatments, plants were normally watered for 7 d of recovery, and then the seed set of plants stressed for different days was determined. At least 3 replicates were performed for each treatment.

Accession numbers

Sequence data from this article can be found in TAIR under the following accession numbers: GSNOR (AT5G43940), SPL (AT4G27330), TT16 (AT5G23260), ES1 (AT5G40260), DD1 (AT1G36340), DD6 (AT2G42930), DD11 (AT1G52970), DD22 (AT5G38330), and DD45 (AT2G21740).

Acknowledgments

We are grateful to Dolf Weijers (Wageningen University) for providing the transgenic line R2D2. We thank Ravi Palanivelu, Xiaoping Gou, and Patrick Treffon for helpful discussions and comments on this manuscript.

Author contributions

J.W., X.G., and S.X. performed most transgenic work, crossing, and plant material preparation. S.X., J.W., X.G., Y.C., J.Z., and T.L. performed the chemical treatments, microscopy observations, and figure design. E.V. and S.X. designed the study. E.V. and S.X. organized the data and wrote the manuscript. All the authors were involved in the revision of the manuscript and approved the final manuscript.

Supplementary data

The following materials are available in the online version of this article.

Supplementary Figure S1. *hot*5 null mutants have short filaments, but pollen germinates like WT (supports Fig. 1).

Supplementary Figure S2. Pollen tube acceptance and callose accumulation of ovules in WT and *hot5* (supports Fig. 2).

Supplementary Figure S3. The average percent of seed set from a delayed pollination assay (supports Fig. 3).

Supplementary Figure S4. The expression of pGSNOR: GSNOR-GFP in the WT background (supports Fig. 4).

Supplementary Figure S5. Localization of GSNOR-GFP fluorescence in CG ovules before and after fertilization (supports Fig. 4).

Supplementary Figure S6. RNA in situ hybridization showing the expression patterns of GSNOR in WT ovules (supports Fig. 4).

Supplementary Figure S7. The expression of different *DD* markers in Col, *hot5-2*, and lines expressing *GSNOR* under control of the *ES1* or *SPL* promoter (supports Fig. 6).

Supplementary Figure S8. The expression of *PIN1* and *PIN3* is inhibited by NO (supports Fig. 7).

Supplementary Figure S9. Delay of FG development by NO associates with decreased PIN expression (supports Fig. 7).

Supplementary Figure S10. Complementation of *hot5-2* with WT *GSNOR-FLAG/GFP* rescues the fertility and other phenotypic defects (supports Fig. 8).

Supplementary Figure S11. Seed set percentage of reciprocal crosses between control and stressed plants (supports Fig. 8).

Supplementary Figure S12. Auxin efflux restores FG development under drought and salt stress (supports Fig. 8).

Supplementary Table S1. Percent of fertile siliques in Col and complemented *hot5-2* lines under salt and drought stress.

Supplementary Table S2. Percent of seed set in Col and complemented *hot5-2* lines under salt and drought stress.

Supplementary Table S3. Percent of ovules at stages FG6 and FG7 in Col and a *pGSNOR:GSNOR-GFP* complemented line under stress with or without auxin treatment.

Supplementary Video S1. GFP fluorescence in ovules of pGSNOR:GSNOR-GFP complemented (CG) lines at FG4 and FG5.

Supplementary Video S2. Merged fluorescence and DIC image of GSNOR-GFP in ovules of CG lines at FG4 and FG5.

Supplementary Video S3. GFP fluorescence in ovules of CG lines at FG6 and FG7.

Supplementary Video S4. Merged fluorescence and DIC image of GSNOR-GFP in ovules of CG lines at FG6 and FG7.

Supplementary Video S5. GFP fluorescence in ovules of CG lines after fertilization.

Supplementary Video S6. Merged fluorescence and DIC image of GSNOR-GFP in ovules of CG lines after fertilization.

Supplementary Video S7. GFP fluorescence in ovules of the Col background after fertilization.

Supplementary Video S8. Merged fluorescence and DIC image of GSNOR-GFP in ovules of the Col background after fertilization.

Supplementary Data Set 1. Percent of fertile siliques in Col-0, *hot5-2*, WS, and *hot5-4* plants after self-pollination.

Supplementary Data Set 2. Percent of fertile siliques in Col-0, *hot5-2*, WS, and *hot5-4* plants after manual pollination.

Supplementary Data Set 3. Percent of seed set in each silique of Col-0, *hot5-2*, WS, and *hot5-4* plants after manual pollination with self-pollen.

Supplementary Data Set 4. Percent of ovules that successfully accepted pollen tubes in Col-0, *hot5-2*, WS, and *hot5-4* as visualized by aniline blue staining.

Supplementary Data Set 5. Percent of ovules that showed abnormal callose deposition in Col-0, *hot5-2*, WS, and *hot5-4* plants.

Supplementary Data Set 6. Percent of ovules exhibiting a GFP signal from different DD markers was compared between Col-0 and *hot5-2* plants.

Supplementary Data Set 7. Percent of ovules at different developmental stages in Col-0 and *hot5-2* plants.

Supplementary Data Set 8. The average percent of seed set in Col-0 and *hot5-2* plants from a delayed pollination assay.

Supplementary Data Set 9. The average percent of ovules at different FG developmental stages after SNP or SNAP, or with cPTIO treatment in Col and *hot5-2* plants.

Supplementary Data Set 10. Percent of seed set in each silique of different transgenic lines.

Supplementary Data Set 11. Percent of ovules with FG development at FG6 and FG7 stages in transgenic plants.

Supplementary Data Set 12. Fluorescence intensity of PIN1::GFP in Col, *hot5-2*, and SNP-treated Col plants at different FG developmental stages.

Supplementary Data Set 13. Fluorescence intensity of PIN3::GFP in Col, *hot5-2*, and SNP-treated Col plants at different FG developmental stages.

Supplementary Data Set 14. Fluorescence intensity of DR5::GFP in Col, *hot5-2*, and SNP-treated Col plants at different FG developmental stages.

Supplementary Data Set 15. Quantification of relative fluorescent signals of R2D2 (DII/mDII) in the FG of Col, *hot5-2*, and SNP-treated Col plants.

Supplementary Data Set 16. Percent of ovules at FG6 and FG7 after NAA, 2,4-D, or IAA treatment in Col and *hot5-2*.

Supplementary Data Set 17. Percent of ovules at FG6 and FG7 after NAA, SNP, or NAA + SNP treatment in Col.

Supplementary Data Set 18. Statistical analysis of seed set before and after stress.

Supplementary Data Set 19. Seed set percentage of reciprocal crosses between control and stressed plants.

Supplementary Data Set 20. Percent of ovules at FG6 and FG7 after exogenous auxin treatment under drought and salt stress.

Supplementary Data Set 21. Auxin efflux restores FG development under drought and salt stress.

Funding

This work was supported by grants from the United States Department of Agriculture (USDA-CSREES-NRI-001030) and US National Science Foundation (MCB 1517046 and MCB 1817985) to E.V. and the National Natural Science Foundation of China (31870298 and 31370318) to S.X.

Conflict of interest statement. The authors declare that they have no conflict of interest. None declared.

Data availability

The data underlying this article are available in the article and in its online supplementary material.

References

- Adamowski M, Friml J. PIN-dependent auxin transport: action, regulation, and evolution. Plant Cell. 2015:27(1):20–32. https://doi.org/10.1105/tpc.114.134874
- **Albertos P, Wagner K, Poppenberger B.** Cold stress signalling in female reproductive tissues. Plant Cell Environ. 2019:**42**(3):846–853. https://doi.org/10.1111/pce.13408

- Arnaud N, Murgia I, Boucherez J, Briat JF, Cellier F, Gaymard F. An iron-induced nitric oxide burst precedes ubiquitin-dependent protein degradation for *Arabidopsis AtFer1* ferritin gene expression. J Biol Chem. 2006:**281**(33):23579–23588. https://doi.org/10.1074/jbc. M602135200
- Bajon C, Horlow C, Motamayor JC, Sauvanet A, Robert D. Megasporogenesis in Arabidopsis thaliana L.: an ultrastructural study. Sex Plant Reprod. 1999:12(2):99–109. https://doi.org/10.1007/s00497 0050178
- Balcerczyk A, Soszynski M, Bartosz G. On the specificity of 4-amino-5-methylamino-2',7'-difluorofluorescein as a probe for nitric oxide. Free Radic Biol Med. 2005:39(3):327–335. https://doi.org/10.1016/j.freeradbiomed.2005.03.017
- **Boavida LC, McCormick S.** Temperature as a determinant factor for increased and reproducible in vitro pollen germination in *Arabidopsis thaliana*. Plant J. 2007:**52**(3):570–582. https://doi.org/10.1111/j.1365-313X.2007.03248.x
- Chen YH, Li HJ, Shi DQ, Yuan L, Liu J, Sreenivasan R, Baskar R, Grossniklaus U, Yang WC. The central cell plays a critical role in pollen tube guidance in Arabidopsis. Plant Cell. 2007:19(11):3563–3577. https://doi.org/10.1105/tpc.107.053967
- Chen R, Sun S, Wang C, Li Y, Liang Y, An F, Li C, Dong H, Yang X, Zhang J, et al. The *Arabidopsis PARAQUAT RESISTANT2* gene encodes an S-nitrosoglutathione reductase that is a key regulator of cell death. Cell Res. 2009:19(12):1377–1387. https://doi.org/10.1038/cr.2009.117
- Christensen CA, King EJ, Jordan JR, Drews GN. Megagametogenesis in *Arabidopsis* wild type and the Gf mutant. Sex Plant Reprod. 1997:**10**(1):49–64. https://doi.org/10.1007/s004970050067
- Clough SJ, Bent AF. Floral dip: a simplified method for *Agrobacterium* mediated transformation of *Arabidopsis thaliana*. Plant J. 1998:**16**(6): 735–743. https://doi.org/10.1046/j.1365-313x.1998.00343.x
- Corpas FJ, Alché JD, Barroso JB. Current overview of S-nitrosoglutathione (GSNO) in higher plants. Front Plant Sci. 2013:4:126. https://doi.org/10. 3389/fpls.2013.00126
- Corpas FJ, Leterrier M, Valderrama R, Airaki M, Chaki M, Palma JM, Barroso JB. Nitric oxide imbalance provokes a nitrosative response in plants under abiotic stress. Plant Sci. 2011:181(5):604–611. https://doi.org/10.1016/j.plantsci.2011.04.005
- Domingos P, Prado AM, Wong A, Gehring C, Feijo JA. Nitric oxide: a multitasked signaling gas in plants. Mol Plant. 2015:8(4):506–520. https://doi.org/10.1016/j.molp.2014.12.010
- **Drews GN, Yadegari R.** Development and function of the angiosperm female gametophyte. Annu Rev Genet. 2002;**36**(1):99–124. https://doi.org/10.1146/annurev.genet.36.040102.131941
- **Duan Q, Kita D, Johnson EA, Aggarwal M, Gates L, Wu HM, Cheung AY.** Reactive oxygen species mediate pollen tube rupture to release sperm for fertilization in *Arabidopsis*. Nat Commun. 2014:**5**(1):3129. https://doi.org/10.1038/ncomms4129
- Duan Q, Liu MJ, Kita D, Jordan SS, Yeh FJ, Yvon R, Carpenter H, Federico AN, Garcia-Valencia LE, Eyles SJ, et al. FERONIA controls pectin- and nitric oxide-mediated male-female interaction. Nature 2020:579(7800):561–566. https://doi.org/10.1038/s41586-020-2106-2
- Fancy NN, Bahlmann AK, Loake GJ. Nitric oxide function in plant abiotic stress. Plant Cell Environ. 2017:40(4):462–472. https://doi.org/10. 1111/pce.12707
- Feechan A, Kwon E, Yun BW, Wang Y, Pallas JA, Loake GJ. A central role for S-nitrosothiols in plant disease resistance. Proc Natl Acad Sci U S A. 2005:102(22):8054–8059. https://doi.org/10.1073/pnas.0501456102
- Frungillo L, Skelly MJ, Loake GJ, Spoel SH, Salgado I. S-nitrosothiols regulate nitric oxide production and storage in plants through the nitrogen assimilation pathway. Nat Commun. 2014:5(1):5401. https://doi.org/10.1038/ncomms6401
- **Guerra D, Ballard K, Truebridge I, Vierling E.** S-Nitrosation of conserved cysteines modulates activity and stability of S-nitrosoglutathione reductase (GSNOR). Biochemistry 2016:**55**(17):2452–2464. https://doi.org/10.1021/acs.biochem.5b01373

- Gupta KJ, Fernie AR, Kaiser WM, van Dongen JT. On the origins of nitric oxide. Trends Plant Sci. 2011:16(3):160–168. https://doi.org/10.1016/j.tplants.2010.11.007
- Hord CL, Chen C, Deyoung BJ, Clark SE, Ma H. The BAM1/BAM2 receptor-like kinases are important regulators of Arabidopsis early anther development. Plant Cell. 2006:18(7):1667–1680. https://doi.org/10.1105/tpc.105.036871
- Ju Y, Yuan J, Jones DS, Zhang W, Staiger CJ, Kessler SA. Polarized NORTIA accumulation in response to pollen tube arrival at synergids promotes fertilization. Dev Cell. 2021:56(21):2938–2951.e6. https://doi.org/10.1016/j.devcel.2021.09.026
- **Lee U, Wie C, Fernandez BO, Feelisch M, Vierling E.** Modulation of nitrosative stress by S-nitrosoglutathione reductase is critical for thermotolerance and plant growth in Arabidopsis. Plant Cell. 2008:**20**(3):786–802. https://doi.org/10.1105/tpc.107.052647
- Li B, Sun C, Lin X, Busch W. The emerging role of GSNOR in oxidative stress regulation. Trends Plant Sci. 2021:26(2):156–168. https://doi.org/10.1016/j.tplants.2020.09.004
- Liao CY, Smet W, Brunoud G, Yoshida S, Vernoux T, Weijers D. Reporters for sensitive and quantitative measurement of auxin response. Nat Methods. 2015:12(3):207–210. https://doi.org/10.1038/nmeth.3279
- **Liu Y, von Wirén N**. Integration of nutrient and water availabilities via auxin into the root developmental program. Curr Opin Plant Biol. 2022:**65**:102117. https://doi.org/10.1016/j.pbi.2021.102117
- **Lohani N, Singh MB, Bhalla PL**. High temperature susceptibility of sexual reproduction in crop plants. J Exp Bot. 2020:**71**(2):555–568. https://doi.org/10.1093/jxb/erz426
- **Lu J, Magnani E.** Seed tissue and nutrient partitioning, a case for the nucellus. Plant Reprod. 2018:**31**(3):309–317. https://doi.org/10.1007/s00497-018-0338-1
- Mansfield S, Briarty L, Erni S. Early embryogenesis in Arabidopsis thaliana. I. The mature embryo sac. Can J Bot. 1991:69(3):447–460. https://doi.org/10.1139/b91-062
- **Márton ML, Cordts S, Broadhvest J, Dresselhaus T**. Micropylar pollen tube guidance by egg apparatus 1 of maize. Science 2005:**307**(5709): 573–576. https://doi.org/10.1126/science.1104954
- Melser C, Klinkhamer PG. Selective seed abortion increases offspring survival in *Cynoglossum officinale* (Boraginaceae). Am J Bot. 2001:**88**(6):1033–1040. https://doi.org/10.2307/2657085
- Meyer KM, Soldaat LL, Auge H, Thulke HH. Adaptive and selective seed abortion reveals complex conditional decision making in plants. Am Nat. 2014:183(3):376–383. https://doi.org/10.1086/675063
- Mishra V, Singh P, Tripathi DK, Corpas FJ, Singh VP. Nitric oxide and hydrogen sulfide: an indispensable combination for plant functioning. Trends Plant Sci. 2021:26(12):1270–1285. https://doi.org/10.1016/j.tplants.2021.07.016
- Okuda S, Tsutsui H, Shiina K, Sprunck S, Takeuchi H, Yui R, Kasahara RD, Hamamura Y, Mizukami A, Susaki D. Defensin-like polypeptide LUREs are pollen tube attractants secreted from synergid cells. Nature 2009:458(7236):357–361. https://doi.org/10.1038/nature07882
- Petrasek J, Mravec J, Bouchard R, Blakeslee JJ, Abas M, Seifertova D, Wisniewska J, Tadele Z, Kubes M, Covanova M, et al. PIN proteins perform a rate-limiting function in cellular auxin efflux. Science 2006:312(5775):914–918. https://doi.org/10.1126/science.1123542
- Schneitz K, Hülskamp M, Pruitt RE. Wild-type ovule development in Arabidopsis thaliana: a light microscope study of cleared whole-mount tissue. Plant J. 1995:7(5):731–749. https://doi.org/10.1046/j. 1365-313X.1995.07050731.x
- **Severino LS**. Plants make smart decisions in complex environments. Plant Signal Behav. 2021:**16**(11):1970448. https://doi.org/10.1080/15592324.2021.1970448
- Shi DQ, Liu J, Xiang YH, Ye D, Sundaresan V, Yang WC. SLOW WALKER1, essential for gametogenesis in Arabidopsis, encodes a WD40 protein involved in 18S ribosomal RNA biogenesis. Plant Cell. 2005:17(8):2340–2354. https://doi.org/10.1105/tpc.105.033563

- Shi YF, Wang DL, Wang C, Culler AH, Kreiser MA, Suresh J, Cohen JD, Pan J, Baker B, Liu JZ. Loss of GSNOR1 function leads to compromised auxin signaling and polar auxin transport. Mol Plant. 2015:8(9): 1350–1365. https://doi.org/10.1016/j.molp.2015.04.008
- Shi H, Ye T, Zhu JK, Chan Z. Constitutive production of nitric oxide leads to enhanced drought stress resistance and extensive transcriptional reprogramming in *Arabidopsis*. J Exp Bot. 2014:**65**(15):4119–4131. https://doi.org/10.1093/jxb/eru184
- Smyth DR, Bowman JL, Meyerowitz EM. Early flower development in Arabidopsis. Plant Cell. 1990:2(8):755–767. https://doi.org/10.1105/tpc.2.8.755
- Steffen JG, Kang IH, Macfarlane J, Drews GN. Identification of genes expressed in the *Arabidopsis* female gametophyte. Plant J. 2007:**51**(2): 281–292. https://doi.org/10.1111/j.1365-313X.2007.03137.x
- Sun K, Hunt K, Hauser BA. Ovule abortion in Arabidopsis triggered by stress. Plant Physiol. 2004:135(4):2358–2367. https://doi.org/10.1104/pp.104.043091
- Vishnyakova M. Callose as an indicator of sterile ovules. Phytomorphology 1991:41:245–252.
- Wang J, Guo X, Xiao Q, Zhu J, Cheung AY, Yuan L, Vierling E, Xu S. Auxin efflux controls orderly nucellar degeneration and expansion of the female gametophyte in *Arabidopsis*. New Phytol. 2021a:230(6): 2261–2274. https://doi.org/10.1111/nph.17152
- Wang Y, Impa SM, Sunkar R, Jagadish SVK. The neglected other half-role of the pistil in plant heat stress responses. Plant Cell Environ. 2021b:44(7):2200–2210. https://doi.org/10.1111/pce.14067
- Xie Y, Mao Y, Lai D, Zhang W, Zheng T, Shen W. Roles of NIA/NR/NOA1-dependent nitric oxide production and HY1 expression in the modulation of *Arabidopsis* salt tolerance. J Exp Bot. 2013:**64**(10): 3045–3060. https://doi.org/10.1093/jxb/ert149
- Xu W, Fiume E, Coen O, Pechoux C, Lepiniec L, Magnani E. Endosperm and nucellus develop antagonistically in Arabidopsis seeds. Plant Cell. 2016:28(6):1343–1360. https://doi.org/10.1105/tpc.16.00041
- Xu SB, Guerra D, Lee U, Vierling E. S-Nitrosoglutathione reductases are low-copy number, cysteine-rich proteins in plants that control multiple developmental and defense responses in *Arabidopsis*. Front Plant Sci. 2013:4:430. https://doi.org/10.3389/fpls.2013.00430
- Yang WC, Shi DQ, Chen YH. Female gametophyte development in flowering plants. Annu Rev Plant Biol. 2010:61(1):89–108. https://doi.org/10.1146/annurev-arplant-042809-112203
- Yang WC, Ye D, Xu J, Sundaresan V. The SPOROCYTELESS gene of *Arabidopsis* is required for initiation of sporogenesis and encodes a novel nuclear protein. Genes Dev. 1999:13(16):2108–2117. https://doi.org/10.1101/gad.13.16.2108
- Yu HJ, Hogan P, Sundaresan V. Analysis of the female gametophyte transcriptome of Arabidopsis by comparative expression profiling. Plant Physiol. 2005:139(4):1853–1869. https://doi.org/10.1104/pp.105.067314
- Yu M, Lamattina L, Spoel SH, Loake GJ. Nitric oxide function in plant biology: a redox cue in deconvolution. New Phytol. 2014:202(4): 1142–1156. https://doi.org/10.1111/nph.12739
- Yu X, Zhang X, Zhao P, Peng X, Chen H, Bleckmann A, Bazhenova A, Shi C, Dresselhaus T, Sun MX. Fertilized egg cells secrete endopeptidases to avoid polytubey. Nature 2021:592(7854):433-437. https://doi.org/10.1038/s41586-021-03387-5
- Zhan N, Wang C, Chen L, Yang H, Feng J, Gong X, Ren B, Wu R, Mu J, Li Y, et al. S-Nitrosylation targets GSNO reductase for selective autophagy during hypoxia responses in plants. Mol Cell. 2018:71(1): 142–154.e6. https://doi.org/10.1016/j.molcel.2018.05.024
- **Zhao Y**. Auxin biosynthesis and its role in plant development. Annu Rev Plant Biol. 2010:**61**:49–64. https://doi.org/10.1146/annurev-arplant-042809-112308
- Zhao P, Zhou XM, Shen K, Liu ZZ, Cheng TH, Liu DN, Cheng YB, Peng XB, Sun MX. Two-step maternal-to-zygotic transition with two-phase parental genome contributions. Dev Cell. 2019:49(6): 882–893.e5. https://doi.org/10.1016/j.devcel.2019.04.016